Acute inflammation sensitizes knee-innervating sensory neurons and decreases mouse digging behavior in a TRPV1-dependent manner.

Sampurna Chakrabarti, Luke A. Pattison, Kaajal Singhal, James R.F. Hockley, Gerard Callejo, and Ewan St. John Smith

Department of Pharmacology, University of Cambridge, Cambridge, UK

Corresponding author: Ewan St. John Smith

Department of Pharmacology, University of Cambridge

Tennis Court Road, Cambridge CB2 1PD

Phone: +44 1223 334048, Fax: +44 1223 334100 Email: es336@cam.ac.uk, Lab URL: https://www.phar.cam.ac.uk/research/Smith

Number of text pages (w tables and figs): 46

Number of figures: 6

Number of tables: 2

Number of Supplementary materials: 2

Abstract

Ongoing, spontaneous pain is characteristic of inflammatory joint pain and reduces an individual's quality of life. To understand the neural basis of inflammatory joint pain, we made a unilateral knee injection of complete Freund's adjuvant (CFA) in mice, which reduced their natural digging behavior. We hypothesized that sensitization of knee-innervating dorsal root ganglion (DRG) neurons underlies this altered behavior. To test this hypothesis, we performed electrophysiological recordings on retrograde labelled knee-innervating DRG neurons and measured responses to a number of electrical and chemical stimuli. We found that 24-hours after CFA-induced knee inflammation, knee neurons show a decreased action potential generation threshold, as well as increased GABA and capsaicin sensitivity, but have unaltered acid sensitivity. The inflammation-induced sensitization of knee neurons persisted for 24-hours in culture, but was not observed after 48-hours in culture. Through immunohistochemistry, we showed that the increased knee neuron capsaicin sensitivity correlated with enhanced expression of the capsaicin receptor, transient receptor potential vanilloid 1 (TRPV1) in the CFA-injected side. We also observed an increase in the co-expression of TRPV1 with tropomyosin receptor kinase A (TrkA), which is the receptor for nerve growth factor (NGF), suggesting that NGF partially induces the increased TRPV1 expression. Lastly, we found that systemic administration of the TRPV1 antagonist A-425619 reversed the decrease in digging behavior induced by CFA injection, further confirming the role of TRPV1, expressed by knee neurons, in acute inflammatory joint pain.

(232 words, limit 250)

Introduction

Pain is protective, but its dysregulation has a negative impact on an individual's life, as well as a wider socioeconomic impact [59,65]. Inflammatory joint pain is characteristic of many musculoskeletal disorders, often being more diffuse and longer lasting than cutaneous pain [42]. Although spontaneous pain is a hallmark of joint pain, most rodent studies focus on evoked pain behaviors [3,53]. Therefore, shifting the emphasis to study natural behaviors during painful conditions and their underlying molecular mechanisms might facilitate the translation of novel analgesics into clinics [3].

A variety of techniques have been employed to better understand the molecular drivers of pain. For example, RNA-sequencing studies have characterized dorsal root ganglia (DRG) neurons into distinct subpopulations [32,43,64], and electrophysiology and immunohistochemistry have shown that joint innervating DRG neurons possess distinct neurochemical and electrophysiological properties [56]. These reports highlight the importance of specifically studying knee neurons, to fully understand the neural basis of joint pain.

Multiple ion channels are involved in transducing noxious stimuli; of these, the Transient Receptor Potential (TRP) channel family are critical to nociceptor chemosensitivity [45]. Alongside endogenous mediators released during inflammation, e.g. protons, we have shown that articular neurons can be activated by the TRP channel agonists capsaicin (TRPV1), cinnamaldehyde (TRPA1) and menthol (TRPM8) [56]. In relation to this, TRPV1$^{-/-}$ and TRPA1$^{-/-}$ mice show reduced pain behavior in CFA models of articular nociception [12,19]. Although not tested after CFA-induced joint inflammation, TRPM8$^{-/-}$ mice develop similar mechanical hyperalgesia to wildtype mice following CFA injection into the footpad [8]. Joint acidosis correlates with increased severity of inflammatory arthritis in humans, and acidic solutions activate

and sensitize rodent nociceptors [18,58]. Mice lacking the proton-gated ion channels acid-sensing ion channel 3 (ASIC3) and TRPV1 have reduced mechanical hyperalgesia following intra-articular CFA injection [35], but not following subcutaneous hind paw CFA injection, suggesting regional differences in pain processing [60]. Subsequently, using magnetic resonance spectroscopic imaging, we found no evidence of tissue acidosis following subcutaneous CFA injection [69], suggesting absence of a key stimulus for ASIC3/TRPV1 activation, hence perhaps explaining the lack of phenotype observed in the hind paw CFA model. However, it remains unknown how proton-gated channels contribute to knee neuron activation during acute inflammation.

Regardless of the stimulus, once activated, sensory neuron input to the spinal cord is pre-synaptically modulated by $GABA_A$ receptor signaling, the source of GABA being spinal cord interneurons [63]. In adults, due to the high intracellular $[Cl^-]$ in DRG neurons compared to central nervous system neurons, activation of $GABA_A$ receptors produces depolarization through $[Cl^-]$ efflux [11]. Furthermore, after subcutaneous CFA-induced inflammation in rat paws, the magnitude of GABA-evoked currents is increased in cutaneous DRG neurons [75], as well as in isolated human DRG neurons incubated in an inflammatory soup [73]. However, the characteristics of GABA-evoked currents in knee neurons, and their modulation during inflammation are unknown.

Here, we hypothesized that sensitization of knee-innervating neurons following CFA-induced knee inflammation underlies changes in natural behavior.

(485 words, limit 500 words)

Methods

Animals

All mice used in this study were 6-15 week old female C57/BL6 (Envigo); female mice were used because being female is a risk factor for inflammatory pain [28]. Mice were conventionally housed in groups of 4-5 with nesting material and a red plastic shelter; the holding room was temperature controlled (21 °C) and mice were on a normal 12 hour/light dark cycle with food and water available *ad libitum.* This research was regulated under the Animals (Scientific Procedures) Act 1986 Amendment Regulations 2012 following ethical review by the University of Cambridge Animal Welfare and Ethical Review Body.

Knee joint intra-articular injections

Under anesthesia (ketamine, 100 mg/kg and xylazine, 10 mg/kg, i.p.) a single injection of the retrograde tracer Fast Blue (FB; 1.5 µl 2% in 0.9 % saline; Polysciences) was made intra-articularly through the patellar tendon into each knee to label knee-innervating neurons. For all experiments, anaesthetized mice were injected with 7.5 µl Complete Freund's adjuvant (CFA; 10 mg/ml; Chondrex) intra-articularly through the patellar tendon in one knee seven days after administration of FB. Knee width was measured with Vernier's calipers before and 24-hours after CFA injection.

Digging behavior paradigm

Digging behavior testing was carried out in a subset of mice used for electrophysiological and immunohistochemistry studies. A standard 49 x 10 x 12 cm cage with a wire lid, filled with

Aspen midi 8/20 wood chip bedding (LBS Biotechnology) tamped down to a depth of ~ 4 cm, was used as the test environment. Each mouse was tested individually using fresh bedding. Testing lasted three minutes and to avoid distractions food and water were not available. All digging experiments were carried out between 12:00 and 14:00 on weekdays in the presence of one male and one female experimenter.

Testing protocol for assessing the impact of CFA-induced inflammation:

Each day before assessment of digging, mice were habituated in the procedure room, in their home cage, for 30 min. On the training days (2 days before FB or CFA injection in the knee, Figure 1A) mice were allowed to dig twice, with a 30-minute break between sessions. All subsequent days were test days and after habituation mice were allowed to dig once. Test digs were recorded and the digging duration (time spent actively displacing bedding material), as well as the number of visible burrows in test cages were counted. Digging duration was scored independently by the two experimenters from video recordings. Since the scores were well correlated (Pearson correlation $R^2 = 0.93$), an average is reported.

Testing protocol for assessing the effect of TRPV1-antagonist, A-425619:

Seventeen mice were trained as above and the day before CFA knee injections their digging behavior was measured twice with a 30 min interval in between. Since the digging duration (saline group: Run 1, 30.3 ± 18.7 s vs. Run 2, 33.8 ± 17.0 s; CFA group: Run 1, 32.2 ± 16.2 s vs. Run 2, 31.1 ± 19.4 s, $p = 0.8$, $n = 10$, $p = 0.7$, $n = 7$, paired t-test) and number of burrows (saline group: Run 1, 3.4 ± 0.9 vs. Run 2, 3.4 ± 0.9; CFA group, Run 1, 4 ± 0.9 vs. Run 2, 4.3 ± 1.2, $p = 0.3$, $n = 10$, $p > 0.9$, $n= 7$, paired t-test) did not change between these two test digs for either group, the measurement from the second run is reported as pre-CFA/saline. On the day of the injection, the

111 mice were randomly split into two groups: the CFA group received CFA in one knee (as described
112 above) and the control group received saline in one knee. 24-hours after the injections, digging
113 activity was re-assessed, after which all mice received an intra-peritoneal dose of the TRPV1
114 antagonist, A-425619 (100 μmol/kg, Tocris, made up in 10% DMSO and 34% 2-hydroxylpropyl
115 β-cyclodextrin, Sigma-Aldrich, in dH_2O). Digging activity was measured again after 30 min as
116 previous reports show maximal anti-nociceptive effect of A-425619 at this time point [31]. At the
117 end of the study all the videos of test digs were independently assessed by the experimenters, who
118 were blinded to the treatment conditions and stage of the experiment by an assistant, and an
119 average of their scores is reported.

120

121 *DRG neuron culture*

122 Following cervical dislocation and decapitation, the spinal column was dissected and the
123 lumbar (L2 to L5) DRG (that primarily innervate the knee joint) were collected [49,56]. DRG from
124 the CFA-injected and non-injected sides were separately collected in ice cold dissociation media
125 containing L-15 Medium (1X) + GlutaMAX-l (Life Technologies), supplemented with 24 mM
126 $NaHCO_3$. DRG were then incubated in 3 ml type 1A collagenase (1 mg/ml with 6 mg/ml bovine
127 serum albumin (BSA) in dissociation media; Sigma-Aldrich) for 15 min at 37 °C, followed by 30
128 min incubation in 3 ml trypsin solution (1 mg/ml with 6 mg/ml BSA in dissociation media; Sigma-
129 Aldrich) at 37 °C. After removing the enzymes, the DRG were suspended in culture media
130 containing L-15 Medium (1X) + GlutaMAX-l, 10 % (v/v) fetal bovine serum, 24 mM $NaHCO_3$,
131 38 mM glucose, 2 % penicillin/streptomycin, dissociated by mechanical trituration with a 1 ml
132 Gilson pipette and briefly centrifuged (160 g, 30 s; Biofuge primo, Heraeus Instruments; Hanau,

133 Germany). Supernatants containing dissociated DRG neurons were then collected in a fresh tube.
134 This was repeated five times. Finally, the cells were plated onto poly-D-lysine and laminin coated
135 glass bottomed dishes (MatTek, P35GC-1.5-14-C) and incubated (37 °C, 5 % CO_2) for 4-, 24- or
136 48-hours depending upon the experiment.

137

138 *Immunohistochemistry*

139 FB labelled and CFA-injected mice were transcardially perfused, firstly with PBS,
140 followed by 4 % (w/v) paraformaldehyde (PFA; in PBS, pH 7.4) under terminal anesthesia
141 (sodium pentobarbital; 200 mg/kg, i.p.). L2 – L5 DRG were collected from the ipsilateral and
142 contralateral sides and post-fixed for 1-hour (4 % PFA), followed by an overnight incubation in
143 30 % (w/v) sucrose (in PBS) at 4 °C for cryoprotection. DRG were next embedded in Shandon M-
144 1 Embedding Matrix (Thermo Fisher Scientific), snap frozen in 2-methylbutane (Honeywell
145 International) on dry ice and stored at -80 °C. Embedded DRG were sectioned (12 μm) using a
146 Leica Cryostat (CM3000; Nussloch, Germany), mounted on Superfrost Plus microscope slides
147 (Thermo Fisher Scientific) and stored at -20 °C until staining. One to three sections were chosen
148 at random for analysis from each CFA-injected and contralateral side of four mice.

149 Slides were defrosted, washed with PBS-tween and blocked in antibody diluent solution:
150 0.2 % (v/v) Triton X-100, 5 % (v/v) donkey serum and 1 % (v/v) bovine serum albumin in PBS
151 for 1-hour at room temperature before overnight incubation at 4 °C with primary antibodies anti-
152 TRPV1 (1:1000, rabbit polyclonal, Abcam ab31895) and anti-TrkA (1:1000, goat polyclonal,
153 R&D systems AF1056) in antibody diluent. Slides were washed three times using PBS-tween and
154 incubated with species-specific conjugated secondary antibodies (1:1000, anti-rabbit Alexa-488

155 (Invitrogen, A21206) and anti-goat Alexa-568 (Invitrogen, A11057)) for 2-hours at room
156 temperature (20-22 °C). Slides were washed in PBS-tween, mounted and imaged with an Olympus
157 BX51 microscope (Tokyo, Japan) and QImaging camera (Surrey, Canada). Exposure levels were
158 kept constant for each slide and the same contrast enhancements were made to all slides. Negative
159 controls without the primary antibody showed no staining with either secondary.

160 Using ImageJ, the mean gray value of each neuron in a DRG section was measured and
161 normalized between the highest and lowest intensity neuron for that section. The threshold used
162 for scoring a neuron as positive for a stain was set as the normalized minimum gray value across
163 all sections + 2 times SD.

164

165 *Whole cell patch-clamp electrophysiology*

166 At least three DRG neurons from the CFA-injected side (CFA) and contralateral (Cntrl)
167 side from each animal were recorded. To try and maintain an even distribution of animals across
168 all time points at which recordings were made, the same culture was used for 4-hours, 24-hours
169 and 48-hours wherever possible, however, due to the paucity of labelled neurons and variability of
170 culture conditions, this was not possible in some cases. In total, each of the conditions contained
171 DRG neurons from 6-8 mice. At each time point recordings were made for-4 hours. The
172 extracellular solution contained (in mM): NaCl (140), KCl (4), $MgCl_2$ (1), $CaCl_2$ (2), glucose (4)
173 and HEPES (10) adjusted to the required pH (> 6.0) with NaOH. For solutions with pH < 6.0, MES
174 was used instead of HEPES. Patch pipettes of 4-9 MΩ were pulled with a P-97 Flaming/Brown
175 puller (Sutter Instruments; Novato, CA, USA) from borosilicate glass capillaries and the
176 intracellular solution used contained (in mM): KCl (110), NaCl (10), $MgCl_2$ (1), EGTA (1),

177 HEPES (10), Na_2ATP (2), Na_2GTP (0.5) adjusted to pH 7.3 with KOH. Recordings were made
178 using a HEKA EPC-10 amplifier (Lambrecht, Germany) and the corresponding Patchmaster
179 software. FB labelled neurons were identified by their fluorescence upon excitation with a 365nm
180 LED (Cairn Research; Faversham, United Kingdom). For all experiments, DRG neurons were held
181 at -60 mV and whole cell currents were acquired at 20 kHz. Only neurons where an action potential
182 (AP) could be evoked in response to current injections and had a resting membrane potential more
183 negative than -40 mV were analyzed. Images of neurons were captured using a 40x objective on a
184 Nikon Eclipse Ti-S microscope and a Zyla 5.5 sCMOS camera (Andor; Belfast, United Kingdom),
185 followed by pixel to μm conversion to calculate their diameter using ImageJ software.

186 **Testing Protocols:**

187 **Action potential generation:** APs were generated by 80 ms current injections of 0-1050 pA in 50
188 pA steps. Threshold, amplitude, half peak duration (HPD) and afterhyperpolarisation duration
189 (AHP) (shown in Figure 2A) were measured using Fitmaster software (HEKA).

190 **Acid sensitivity and TRP-agonist sensitivity:** Solutions for determining acid sensitivity (pH 7,
191 pH 6, pH 5) and TRP-agonist sensitivity (capsaicin, cinnamaldehyde and menthol) were applied
192 in a random order to DRG neurons in 5 s pulses with at least 30 s wash period (with pH 7.4)
193 between stimuli. Solutions of 10 μM capsaicin (1 mM stock in 100% ethanol; Sigma-Aldrich),
194 100 μM cinnamaldehyde (10 mM stock in 100% ethanol; Merck) and 100 μM menthol (20 mM
195 stock in 100% ethanol; Alfa Aesar) were made up in pH 7.4 extracellular solution from their
196 respective stock solutions. Current amplitude was measured in Fitmaster (HEKA) by subtracting
197 the maximum peak response from the baseline (average of the first 3 s before stimulation), which
198 was then normalized by dividing by neuron capacitance to give current density.

199 **GABA sensitivity:** 100 μM GABA (100 mM stock in water; Sigma-Aldrich) was applied for 5 s
200 followed by a 20 s wash with pH 7.4, then 100 μM GABA and 250 μM bicuculline (100 mM in
201 DMSO; Sigma-Aldrich) were applied together for 5 s. Recovery from bicuculline block was
202 assessed after 1 min by a subsequent 100 μM GABA application for 5 s. To test for the presence
203 of the $GABA_A$-δ subunit, 100 μM of the δ agonist 4,5,6,7-tetrahydroisoxazolo[5,4-c]pyridin-3-ol
204 hydrochloride (THIP, 100 mM stock in water; Sigma-Aldrich) was applied for 5 s.
205
206 *Statistical Analysis*
207 Comparison of CFA and Cntrl neuron electrophysiological properties was performed using
208 a Student's unpaired t-test (two-sided), while comparison across time (4-hours, 24-hours and 48-
209 hours) was made using a one-way ANOVA followed by a Holm-Sidak multiple comparison test.
210 To compare proportions in patch-clamp and immunostaining experiments, a chi-squared test was
211 used. Knee width before and after inflammation with CFA was compared using a Student's paired
212 t-test (two-sided). Digging behavior of mice in different groups was compared using a repeated
213 measures one-way ANOVA followed by a Holm-Sidak multiple comparison test. Data are
214 presented as mean ± standard deviation.
215
216
217
218
219

220 Results

221 *Inflammation and reduced well-being in mice after unilateral knee joint CFA injection*

222 Injection of CFA into the knee joint produces acute and chronic inflammatory pain in mice
223 that models human arthritis [26]. To produce acute inflammation, 7-days after labelling knee-
224 innervating neurons by FB injection, CFA was injected into the left knee joint of mice (Figure 1A).
225 After 24-hours, we observed robust swelling indicative of edema and inflammation of the
226 ipsilateral knee (pre-CFA, 3.8 ± 0.3 mm vs. post-CFA, 4.6 ± 0.3 mm, $p < 0.0001$, n = 17, paired t-
227 test), but not the contralateral knee (pre-CFA, 3.7 ± 0.3 mm vs. post-CFA, 3.7 ± 0.2 mm, n =17, p
228 > 0.9, paired t-test, Figure 1B, 1C); a pilot study found that FB injection alone induced no change
229 in knee width (n = 6, pre-FB, 3.9 ± 0.1 mm, post-FB, 4.0 ± 0.1 mm, p = 0.4, paired t-test)

230 Spontaneous pain is one of the most distressing features of arthritic conditions that reduces
231 the overall feeling of well-being [24,29] and it has been suggested that burrowing and digging
232 behaviors function as indicators of well-being in mice, such that a reduction in burrowing behavior
233 during inflammatory pain indicates diminished well-being [15,38]. Based on this hypothesis, we
234 measured digging behavior in a subset of mice (n = 7, timeline Figure 1A, see Video,
235 Supplementary Digital Content 1, which demonstrates post-FB and post-CFA of a mouse). During
236 a 3-minute test period, neither the time spent digging (pre-FB, 45.8 ± 15.8 s vs. post-FB, 39.8 ±
237 12.4 s, t = 1.1, ANOVA, Holm-Sidak's multiple comparison test, Figure 1D), nor the number of
238 burrows dug (pre-FB, 3.8 ± 0.7 vs. post FB, 3.7 ± 0.5, t = 0.5, ANOVA, Holm-Sidak's multiple
239 comparison test, Figure 1E) was altered following FB injection. However, CFA injection resulted
240 in decreased digging time (pre-CFA, 52.7 ± 23.9 s vs. post-CFA, 17.9 ± 18.4 s, p = 0.003, t = 3.9,
241 ANOVA, Holm-Sidak's multiple comparison test, Figure 1D) and a decreased number of burrows
242 dug (pre-CFA, 4.3 ± 0.5 vs. post-CFA, 2.1 ± 0.9, p = 0.0003, t = 6.3, ANOVA, Holm-Sidak's

243 multiple comparison test, Figure 1E), suggesting a significant impact to well-being, elicited by
244 joint inflammation. Comparison of post-FB and post-CFA time points also showed that CFA-
245 injection produced a reduction in the time spent digging ($p = 0.003$, $t = 4.8$, ANOVA, Holm-
246 Sidak's multiple comparison test) and in the number of burrows dug ($p = 0.0003$, $t = 4.2$, ANOVA,
247 Holm-Sidak's multiple comparison test).

248

249 *Action potential threshold of knee neurons decreases after intra-articular CFA injection.*

250 To determine if altered sensory input may underlie the inflammation-induced decrease in
251 digging behavior observed, we characterized the electrical properties of knee-innervating DRG
252 neurons isolated from mice undergoing unilateral CFA knee injection as above (CFA neurons);
253 DRG neurons innervating the contralateral knee were used as control (Cntrl neurons). *In vivo*
254 recordings from rat joint afferents have shown increased excitability during inflammation [27].
255 Therefore, we hypothesized that AP threshold would decrease in mouse knee neurons following
256 CFA-injection.

257 We recorded electrically-evoked APs from CFA neurons (Figure 2A) (CFA, $n = 25$) and
258 Cntrl neurons ($n = 27$) with similar diameters (Figure 2B, Table 1) after 4-hours in culture. The
259 AP threshold of CFA neurons was ~ 30 % lower compared to Cntrl neurons ($p = 0.01$, unpaired t-
260 test) (Figure 2C, Table 1), suggesting hyperexcitability and sensitization of these neurons. By
261 contrast, there was no change in the HPD ($p = 0.3$, unpaired t-test, Figure 2D) or amplitude ($p =$
262 0.7, unpaired t-test, Table 1) of the electrically-evoked APs following inflammation, whilst the
263 AHP increased ($p = 0.009$, unpaired t-test, Figure 2E).

264

265 *Acid-sensitivity does not change in knee neurons following inflammation.*

266 Tissue acidosis occurs in some forms of inflammation in humans [18,23], and in rodents
267 there are also contrasting findings [2,69]. We used a range of pH solutions to determine if knee
268 neuron acid-sensitivity changes following knee CFA injection. Depending upon the pH stimulus
269 used, virtually all neurons responded with an inward current (pH 7 = 80.6 ± 4.6 %, pH 6 = 98.0 ±
270 2.0 % and pH 5 = 100 %). A small proportion of neurons showed a rapidly activating transient
271 inward current followed by a sustained phase (transient + sustained) at pH 6 and pH 5. These
272 currents were likely mediated by acid-sensing ion channels (ASICs) and their frequency was
273 unaltered in CFA neurons (CFA, 16.3 ± 3.7 %; Cntrl, 11.1 ± 3.7 %, combined mean of pH 6 and
274 pH 5) (Figure 3A, 3B). Sustained currents were the dominant response at all the pH tested (Figure
275 3A, C) and no difference was observed in the amplitude of response to any pH stimulus between
276 CFA and Cntrl neurons (Figure 3D-F, Table 2). Overall, this suggests that there was no significant
277 change in acid sensitivity in articular neurons during acute inflammation.

278

279 *Inflammation increases the proportion of TRPV1 expressing knee neurons.*

280 Sensory neurons express a variety of TRP channels involved in thermo- and chemosensing
281 and these are both activated and sensitized by a range of inflammatory mediators [45]. To
282 determine if any change in TRP-mediated chemosensitivity occurs in knee neurons following acute
283 inflammation, we tested 10 μM capsaicin, 100 μM cinnamaldehyde and 100 μM menthol, agonists
284 of TRPV1, TRPA1 and TRPM8 respectively.

285 The percentage of capsaicin-sensitive CFA neurons increased significantly compared to
286 Cntrl neurons (CFA, 72 % vs. Cntrl, 44 %, p = 0.02, chi-sq test, Figure 4A). However, there was

287 no change in the peak current density of capsaicin-evoked currents ($p = 0.3$, unpaired t-test, Table
288 2). By contrast, no change in the percentage of cinnamaldehyde-sensitive (CFA, 40 %, Cntrl, 67
289 % $p = 0.06$; chi-sq test, Figure 4B) or menthol-sensitive neurons (CFA, 35 %, Cntrl, 51 %, $p = 0.2$,
290 chi-sq test, Figure 4C) was observed, nor was there any difference in the peak current density of
291 either cinnamaldehyde- or menthol-evoked currents following inflammation (Table 2,
292 cinnamaldehyde, $p = 0.1$; menthol, $p = 0.8$, unpaired t-test). An increased proportion of knee DRG
293 neurons responding to capsaicin in inflammation suggests recruitment of a previously capsaicin
294 "silent" population (Figure 4D).

295 To confirm that an increase in the proportion of capsaicin sensitive knee neurons is due to
296 increased TRPV1 expression, we conducted immunohistochemistry on whole DRG sections (L2-
297 L5) from ipsilateral (CFA, n = 1089 neurons) and contralateral (Cntrl, n = 1334 neurons) sides of
298 four mice (Figure 4Ei). A significantly higher proportion of CFA neurons displayed TRPV1
299 expression (59.7%) compared to Cntrl neurons (44.6 %, $p < 0.0001$, chi-sq test, Figure 4Eii). Nerve
300 growth factor (NGF) is an important inflammatory mediator implicated in arthritis that binds to its
301 high affinity receptor tropomyosin receptor kinase A (TrkA) and can increase TRPV1 expression
302 [37]. Hence, we hypothesized that the increased TRPV1 expression observed will occur in TrkA
303 positive neurons, leading to increased TRPV1 and TrkA coexpression. Although, the proportion
304 of knee neurons expressing TrkA (CFA, 39.3 %, Cntrl, 42.6 %) (Figure 4Eii) was not greater in
305 CFA neurons than Cntrl neurons, there was a small, yet significant, increase in the proportion of
306 CFA neurons co-expressing TRPV1 and TrkA compared to Cntrl neurons (CFA, 24.8 %; Cntrl,
307 29.8 %, $p = 0.02$, chi-sq test, Figure 4Eii). Taken together, our data suggests that NGF-TrkA
308 signaling contributes, alongside as yet unknown pathways, to driving increased TRPV1 expression
309 following CFA.

310

311 *Sustained $GABA_A$-evoked current magnitude increases in knee neurons following inflammation.*

312 An inflammation-induced increase in amplitude of GABA-evoked currents has been
313 reported in skin-labeled rat DRG neurons, suggesting that altered GABAergic signaling may be
314 important in inflammatory pain [75]. We observed that 100 μM GABA evoked a response in 76
315 % of CFA and 96 % of Cntrl neurons ($p = 0.03$, chi-sq test). Two types of GABA response were
316 observed. In the first, the current reached a peak within 1.5 s of GABA application and was
317 classified as transient + sustained (TS). Two subtypes of TS responses were observed: one showing
318 relatively monophasic desensitization throughout GABA application (Figure 5Ai) and a second
319 showing a far slower desensitization that produced a more stable sustained phase (Figure 5Aii);
320 due to the paucity of neurons in the first subgroup and since no response returned to baseline within
321 5 s, both types were included in the TS group. The second type of GABA-evoked response did
322 not reach its peak within the first 1.5 s, showed no desensitization and was classified as sustained
323 (S, Figure 5Aiii). The frequency of TS and S responses in CFA and Cntrl neurons was similar
324 (CFA: TS, 48 %, S, 28 % vs. Cntrl: TS, 52 %, S, 44 %, Figure 5 Bi). Although no difference in
325 GABA-evoked peak current density was observed overall between CFA and Cntrl neurons (Figure
326 5Bii, Table 2), GABA-evoked S type currents were of larger magnitude in CFA than Cntrl neurons
327 (CFA, 8.0 ± 10.7 pA/pF, n =7 vs. Cntrl, 1.1 ± 2.5 pA/pF, n = 14, $p = 0.03$, unpaired t-test), whereas
328 no such difference was observed for TS type currents (CFA, 6.7 ± 8.5 pA/pF, n =12 vs. Cntrl, 6.5
329 ± 6.8, n = 12, $p = 0.5$, unpaired t-test) (Figure 5Biii).

330 Due to inflammation producing an increase in the magnitude of S type GABA-evoked
331 currents, we investigated the subunit composition of these GABA receptors. The $GABA_A$
332 antagonist, bicuculline, inhibited GABA responses by more than 50 % in 6/7 CFA DRG and 8/12

333 Cntrl DRG (Figure 5Ci), with all GABA-evoked currents being sensitive to bicuculline to some
334 extent. These results concur with the previous observation that a fraction of GABA-evoked
335 currents in rat DRG neurons is bicuculline insensitive [41]. S type $GABA_A$ currents can be
336 mediated by δ subunit containing $GABA_A$ receptors [41] and thus we tested the ability of the δ
337 subunit containing $GABA_A$ receptor agonist THIP to evoke currents in knee neurons. A sustained
338 current in response to THIP was observed in 4/8 CFA and 6/11 Cntrl neurons, indicating
339 expression of δ-subunit containing $GABA_A$ receptors in knee neurons (Figure 5Ci, Cii). The peak
340 current density of THIP-evoked currents was similar ($p = 0.9$, unpaired t-test) in CFA (0.6 ± 0.4
341 pA/pF) and Cntrl (0.5 ± 0.3 pA/pF) neurons. However, not all the neurons with S type GABA
342 response showed THIP sensitivity. Combined with the presence of bicuculline insensitive currents,
343 the lack of response to THIP in all neurons with S currents suggests expression of either ρ subunit
344 containing $GABA_A$ receptors, or perhaps $GABA_B$ receptors, both of which produce sustained
345 currents in response to GABA [10]. Taken together, our data indicates the presence of diverse
346 $GABA_A$ receptor subunits in CFA and Cntrl neurons and demonstrates an increase in GABA-
347 mediated neuronal excitation following knee inflammation.
348
349 *Time-in-culture leads to loss of inflammation-induced sensitization of knee neurons.*
350 The period of time that neurons are left in culture for (time-in-culture) and constituents of
351 the culture medium can greatly alter neuronal excitability [54,68]. To systematically characterize
352 the effect of time-in-culture in our system, we repeated the experiments described above on the
353 CFA and Cntrl knee neurons after 24-hours (CFA, n = 25; Cntrl, n = 22) and 48-hours (CFA, n =
354 23; Cntrl, n = 22) in culture.

355 No change was observed in the resting membrane potential, capacitance (Table 1) or AP
356 amplitude (Table 1, CFA, p = 0.4, Cntrl, p = 0.06, ANOVA) across the 3 time points. By contrast,
357 whereas the AP threshold was similar across time points for CFA knee neurons (p = 0.06,
358 ANOVA), it decreased for Cntrl neurons after 48-hours in culture compared to 24-hours (p = 0.03,
359 ANOVA, Holm-Sidak multiple comparison test, Table 1). Interestingly, the inflammation-induced
360 decrease in AP threshold of CFA neurons compared to Cntrl neurons that was observed at 4-hours
361 (Figure 2C) and 24-hours (p = 0.002, unpaired t-test, Table 1) had disappeared after 48-hours in
362 culture (Table 1, p = 0.44, unpaired t-test), which suggests that time-in-culture leads to a loss of
363 inflammation-induced hyperexcitability. There was also a distinct AP widening characterized by
364 an increase in both HPD and AHP in the 48-hours group for Cntrl neurons, but just the HPD in
365 CFA neurons. HPD increased by ~ 60 % after 48-hours in both CFA (p = 0.01, ANOVA) and Cntrl
366 (p = 0.007, ANOVA) neurons compared to the 4-hours group (Table 1). In Cntrl neurons, AHP
367 increased by 191 % in the 48-hours group compared to 4-hours and 81 % compared to 24-hours
368 group (p = 0.0002, ANOVA, Holm-Sidak multiple comparison test, Table 1). One CFA and one
369 Cntrl neuron in the 48-hours culture group were excluded from this analysis because of a highly
370 different AP waveform that could not be analyzed using the same measurements.

371 With regards to knee neuron acid sensitivity, the percentage of neurons with transient +
372 sustained currents in response to pH 6 and pH 5 at 24-hours and 48-hours (see Figure,
373 Supplementary Digital Content 2A showing time-in-culture effects on acid of knee neurons after
374 inflammation) was similar to that at 4-hours (Figure 3A). Although a largely reversible increase in
375 pH 7- (CFA and Cntrl) and pH 5-evoked (Cntrl) current amplitude was observed at 24-hours (pH
376 7: CFA, p = 0.005; Cntrl, p = 0.0003, ANOVA; pH 6: CFA, p = 0.06; Cntrl, p = 0.08, ANOVA;

377 and pH 5: CFA, p = 0.06; Cntrl, p = 0.008, ANOVA) (Table 2), there was no clear trend across
378 different pH stimuli for either CFA or Cntrl neurons.

379 For knee neuron TRP-mediated chemosensitivity, the CFA-induced increase in the
380 proportion of capsaicin-sensitive neurons observed at 4-hours was maintained at 24-hours (CFA,
381 88 % vs. Cntrl, 50%, p = 0.004, chi-sq test), but was absent in the 48-hours group (CFA, 54.2 %
382 vs. Cntrl, 43.5 %, p = 0.5, chi-sq test), a result that further confirms our observations that after 48-
383 hours in culture the inflammation-induced effects are lost. In addition, the proportion of
384 cinnamaldehyde (CFA, 33.3 %; Cntrl, 21.7 %) and menthol-sensitive (CFA, 33.3 %; Cntrl, 13.0
385 %) neurons after 48-hours in culture decreased compared to the other two time points, although
386 this decrease was only significant in Cntrl neurons (cinnamaldehyde, p = 0.0006; menthol, p =
387 0.005, chi-sq test) (see Figure, Supplementary Digital Content 2B, showing time-in-culture effects
388 on TRP agonist of knee neurons after inflammation). No significant difference in the peak current
389 density of TRP agonist-evoked currents was observed across time-in-culture (Table 2).

390 When GABA-evoked currents were split into TS and S types, no changes in the peak
391 current density were observed between CFA and Cntrl after 24-hours or 48-hours in culture.
392 However, combining both TS and S currents, CFA neurons had larger amplitude GABA-evoked
393 currents than Cntrl neurons after 24-hours in culture (p = 0.01, unpaired t-test, Table 2); an effect
394 that was not seen in the 48-hours group (p = 0.2, unpaired t-test, Table 2). Previously, it has been
395 shown in cultured rat DRG neurons that the proportion of S type GABA-evoked currents increased
396 with time-in-culture [41], a result replicated here in mouse knee neurons (CFA, p = 0.03, Cntrl, p
397 = 0.02, chi-sq test, see Figure, Supplementary Digital Content 2C, showing time-in-culture effects
398 on GABA sensitivity of knee neurons after inflammation). From this data, we would recommend

399 not using DRG neurons for longer than 28-hours in culture to prevent loss of inflammation-induced
400 sensitization events.

401

402 *TRPV1 inhibition reverses inflammation induced decrease in digging behavior.*

403 From our characterization of CFA and Cntrl neurons, knee neuron TRPV1 expression
404 emerged as an important target in CFA-induced knee inflammation. We hypothesized that TRPV1
405 underlies our observed knee inflammation-induced decrease in digging behavior observed in mice
406 and that the TRPV1 antagonist A-425619 would thus reverse this decrease. On day 2 of our
407 experimental timeline (Figure 6A), both the CFA group (n = 10) and saline group (n = 7) spent a
408 similar amount of time digging (CFA, 31.1 ± 19.4 s; Saline, 33.8 ± 17.0 s) and produced a similar
409 number of burrows (CFA, 4.3 ± 1.2; Saline, 3.4 ± 0.9). Following CFA/saline injection, the CFA
410 group showed an expected decrease in digging duration (17.4 ± 16.4 s, $p = 0.001$, $t = 3.6$, ANOVA,
411 Holm-Sidak multiple comparison test, Figure 6B), which was reversed 30 min after the injection
412 of A-425619 (36.4 ± 22.2 s, $p = 0.001$, $t = 3.9$, ANOVA, Holm-Sidak multiple comparison test,
413 Figure 6B). A similar result was also obtained with the number of burrows (post-CFA, 2.1 ± 1.0,
414 $p < 0.0001$, $t = 5.0$; post-Ant, 4.0 ± 0.6, $t = 5.7$, ANOVA, Holm-Sidak multiple comparison test,
415 Figure 6C). In contrast, the saline group did not show a decrease in digging behavior 24-hours
416 after saline injection into the knee (Digging duration, 33.1 ± 14.0 s, $p = 0.5$; # Burrows, 3.7 ± 1.4,
417 $p = 0.7$, ANOVA, Figure 6D, 6E), further confirming that intra-articular injections do not affect
418 digging behavior. The TRPV1 antagonist A-425619 also produced no effect on digging behavior
419 in the saline group (Digging duration, 25.9 ± 16.6 s, $p = 0.5$; # Burrows, 3.3 ± 1.1, $p = 0.7$, ANOVA,
420 Figure 6D, 6E), i.e. inhibiting TRPV1 does not interfere with spontaneous digging activity of mice.

421 These results confirm that TRPV1 is an important mediator of inflammatory knee pain and
422 contributes to the inflammation-induced decrease in digging behavior in mice.
423
424
425
426
427
428
429
430
431
432
433
434
435
436
437
438
439

440 *Discussion*

441 CFA evokes both acute (within 18 hours) and chronic (> 6 weeks) inflammatory pain
442 [35,39], as demonstrated by altered evoked-pain behaviors, such as hot/cold plate tests. However,
443 such evoked-pain tests are neither ethologically relevant to rodents, nor model experience of
444 human chronic pain [48]. Consequently, innate rodent behaviors, such as burrowing, digging and
445 nest-building that seek to mirror human activities of daily living have been explored as pain assays
446 [15,38]. A decrease in burrowing behavior has been used to assess pain-like behavior after CFA-
447 induced knee inflammation in rats [50] and digging is a similar innate behavior that is quick and
448 easy to test in a laboratory [15]. Here we show that 24-hours after CFA-induced knee
449 inflammation, mice spent significantly decreased time digging, suggesting that digging can be used
450 as an ethologically relevant pain assay in mice; importantly, intra-articular injection of the
451 retrograde tracer FB did not alter digging behavior.

452 To study the neural basis for the inflammation-induced change in behavior observed, we
453 combined electrophysiology with retrograde labelling of the knee joints, i.e. those neurons exposed
454 to the inflammatory insult. We found that knee neurons have a decreased AP threshold and
455 increased AHP following CFA-induced knee inflammation. The recorded increased AHP in CFA
456 neurons is perhaps contradictory because an increase in current mediated by hyperpolarization-
457 activated cyclic nucleotide-gated ion channels (HCN), and thus a decrease in AHP, is associated
458 with repetitive firing, as shown by one study in trigeminal ganglia neurons after CFA-induced
459 inflammation [22]. However, other studies using CFA-induced hind limb inflammation either
460 observed no change in AHP (like our data at 24-hours in culture) [17] or reported a decrease in
461 AHP only in C-fibers [66]. Therefore, our data possibly demonstrates the multifaceted nature of

462 the molecular mechanisms regulating AHP, a suggestion supported by the wide range of AHP
463 values reported [16,40].

464 TRP channels are cellular sensors of thermal, physical and chemical stimuli [45] and
465 inflammatory mediators released during joint pain can sensitize TRP channels [71]. TRPV1 [72],
466 TRPA1 [61] and TRPM8 [5] are expressed in nociceptors and are involved in hyperalgesia.
467 However, the role of TRPV1 and TRPA1 in acute inflammatory joint pain is unclear. Some studies
468 report that TRPV1$^{-/-}$ mice do not develop CFA- [39] or carrageenan- [14] induced hyperalgesia
469 and others have shown that in DRG neurons TRPV1 protein expression increases in CFA-induced
470 inflammation [1,37,70]. In direct contrast, other studies failed to show increased neuronal TRPV1
471 protein [4,74] or mRNA expression [37] following CFA-induced inflammation. Similarly,
472 TRPA1$^{-/-}$ mice show normal development of CFA-induced hyperalgesia in some studies [20,46],
473 whereas others report attenuation of CFA- and carrageenan-induced hyperalgesia in TRPA1$^{-/-}$ mice
474 [25,44] or following administration of a TRPA1 antagonist [6,51]. We provide
475 electrophysiological evidence that the proportion of capsaicin-sensitive knee neurons increases
476 during acute inflammation from ~ 50% to ~80%, suggesting recruitment of a previously silent
477 neuronal population. We validate this electrophysiology result through immunohistochemistry,
478 demonstrating a similar magnitude increase in the proportion of TRPV1 expressing knee neurons;
479 the observed TRPV1 expression in contralateral knee-innervating neurons reported here agrees
480 with previous findings in rodents [13]. Multiple mechanisms may contribute to this process, for
481 example, NGF released from a variety of cell types in arthritic joints may bind to TrkA and get
482 retrogradely transported to DRG neurons to drive TRPV1 expression. Indeed, increased levels of
483 NGF are found in rheumatic diseases and anti-NGF/TrkA therapy reduces arthritic pain in human
484 and animal models (reviewed in [55]). With regard to CFA-induced pain, it has been previously

485 shown that the proportion of TrkA-expressing neurons innervating bone does not increase
486 following CFA-induced bone pain [52] . We also observed no change in TrkA expression, but did
487 observe a slight, yet significant, increase in TrkA-TRPV1 co-expression following knee
488 inflammation which suggests that NGF-TrkA signaling plays a role in the increased TRPV1
489 expression observed here.

490 Protons are algogens detected by sensory neurons through a variety of means, including
491 ASICs, TRPV1, background K^+ channels, chloride channels and proton-sensing G-protein coupled
492 receptors [33]. There is conflicting evidence surrounding the role of ASICs in inflammatory pain,
493 some studies showing no change, others decreased pain and still others increased pain [47,57]. In
494 terms of joint inflammation, ASIC3$^{-/-}$, TDAG8$^{-/-}$ (a proton-sensing GPCR) and TRPV1$^{-/-}$ mice
495 showed decreased hyperalgesia in an ankle inflammation model [35]. In addition, Ikeuchi *et al*
496 [36] observed upregulation of ASIC3 immunoreactivity in knee-innervating DRG neurons after
497 carrageenan-induced acute knee inflammation in mice. By contrast, ASIC1, ASIC2 and ASIC3
498 knockout mice did not display attenuated thermal or mechanical hyperalgesia after intraplantar
499 CFA injection, suggesting that these ASIC subunits play no role in cutaneous CFA-induced
500 hyperalgesia [60]. We evaluated direct proton activation of knee neurons and found that acid-
501 evoked currents are neither enhanced, nor is there any change in the proportion of ASIC-like
502 currents, following CFA-induced knee inflammation, results that might explain the lack of
503 phenotype observed in certain studies.

504 Information transfer from peripheral to central afferents is modulated by GABAergic
505 signaling. Although an inhibitory neurotransmitter in the central nervous system, GABA produces
506 membrane depolarization through Cl^- efflux in DRG neurons owing to the relatively high
507 intracellular [Cl^-] [62]. GABA-evoked currents in sensory neurons are predominantly $GABA_A$

508 receptor mediated, (identified by their sensitivity to $GABA_A$ antagonist, bicuculline) with diverse
509 subunit composition [41]. As shown previously in rat DRG neurons [41], we recorded both
510 transient and sustained GABA-evoked currents from mouse knee neurons that were largely
511 inhibited by the $GABA_A$ antagonist bicuculline. In addition, our finding that approximately half
512 of all knee neurons were activated by the $GABA_A$-δ subunit agonist, THIP, suggests common
513 expression of the δ-subunit, although the proportion of THIP-activated neurons did not change
514 after CFA injection. The fact that bicuculline did not completely abolish GABA-evoked currents
515 indicates the likely presence of ρ subunits in $GABA_A$ receptors, as has previously been reported
516 in rat DRG neurons [41], or the presence of $GABA_B$ receptor expression (both ρ containing
517 $GABA_A$ receptors and $GABA_B$ receptors are insensitive to bicuculline block). Under normal
518 conditions, GABA-mediated excitation of primary afferent neurons causes primary afferent
519 depolarization, an inhibitory action due to inducing inactivation of voltage gated sodium channels
520 (i.e. depolarizing block). However, following tissue injury, primary afferent depolarization is
521 larger and can actually generate AP to produce pain by excitation of presynaptic $GABA_A$ receptors
522 [9,67]. In this study, we found a decrease in number of GABA responsive CFA neurons, but an
523 increase in the magnitude of GABA-evoked currents compared to Cntrl neurons indicating a
524 potential $GABA_A$ mediated decrease in presynaptic inhibition and an increase in presynaptic
525 excitation.

526 Furthermore, we addressed how time-in-culture affects the electrophysiological properties
527 of neurons isolated from mice undergoing CFA-induced inflammation. Acutely dissociated DRG
528 neurons have been extensively studied with patch clamp electrophysiology, however the definition
529 of "acute" varies. While some studies have recorded within 8-hours of dissection, it is more
530 common to record after overnight incubation (18–28-hours). This variability can potentially

531 confound results on inflammation-induced sensitization, as AP properties change with time-in-
532 culture. Here we show AP broadening, and a slight decrease in AP threshold in neurons from the
533 contralateral side as reported before during a similar time course [54]. We also show that time-in-
534 culture does not affect inflammation-induced lowering of AP threshold up to 28-hours in culture,
535 but that the lowered threshold is lost at 48-hours in culture. Understanding how time-in-culture
536 alters neuronal excitability is important for correctly designing studies. For example, we (present
537 study) and others [41] have shown that S type GABA-evoked responses increase in prevalence
538 with time-in-culture. The present study also shows a decline in the frequency of response to
539 capsaicin, cinnamaldehyde and menthol and the inflammation-induced increase in frequency of
540 capsaicin-sensitive neurons, although maintained for up to 28-hours in culture is lost after 48-
541 hours. By contrast, acid-sensitivity remained relatively stable across all time points.

542 In summary, we show that following unilateral acute inflammation of the knee, knee
543 neurons have 1) a lower AP threshold 2) increased sensitivity to capsaicin and expression of
544 TRPV1 and 3) an increasing trend in the magnitude of GABA-evoked currents up to 28-hours in
545 culture. This specific sensitization signature of knee neurons highlights the importance of studying
546 DRG neurons as a spatially heterogeneous group. Among these different modes of sensitization
547 that likely contribute to the decreased mouse digging behavior following knee inflammation, an
548 increase in TRPV1 function is perhaps most clinically relevant to inflammatory arthritis (reviewed
549 in [21]). Indeed, it has recently been shown that intra-articular administration of a TRPV1
550 antagonist attenuated early osteoarthritic pain in a mono-sodium iodoacetate model [30].
551 Historically in pre-clinical models, TRPV1 antagonists attenuated thermal hyperalgesia, but their
552 efficacy in mechanical hyperalgesia and ongoing pain is unclear [7]. The peripherally restricted
553 TRPV1 antagonist, A-425619, has been previously shown to reverse thermal and mechanical

554 hypersensitivity in rat CFA models and also restore weight bearing ability in rat osteoarthritis
555 models [34]. Here we report that systemic administration of A-425619 is also able to restore the
556 reduction in spontaneous digging behavior in mice brought about by CFA-induced knee
557 inflammation, which further establishes TRPV1 as an important drug target in inflammatory joint
558 pain.

559 (1491 words, limit 1500)

560

561

562

563

564

565

566

567

568

569

570

571

572

Acknowledgments

The authors would like to thank Julie Gautrey and Chris Cardinal for technical assistance with animal work. This work was supported by an Arthritis Research UK Grant (G.C. and E.St.J.S., RG 20930), a Rosetrees Postdoctoral Grant (J.R.F.H. and E.St.J.S., A1296), S.C. was supported by a Gates Cambridge Trust scholarship and L.A.P. was supported by the University of Cambridge BBSRC Doctoral Training Programme (BB/M011194/1).

The authors declare no conflict of interest regarding information in the present report.

590 References

591 [1] Amaya F, Oh-hashi K, Naruse Y, Iijima N, Ueda M, Shimosato G, Tominaga M, Tanaka
592 Y, Tanaka M. Local inflammation increases vanilloid receptor 1 expression within distinct
593 subgroups of DRG neurons. Brain Research 2003;963:190–196.

594 [2] Andersson SE, Lexmuller K, Johansson A, Ekstrom GM. Tissue and intracellular pH in
595 normal periarticular soft tissue and during different phases of antigen induced arthritis in
596 the rat. J Rheumatol 1999;26:2018–2024.

597 [3] Arendt-Nielsen L. Joint pain: more to it than just structural damage? PAIN 2017;158.

598 [4] Bär K-J, Schaible H-G, Bräuer R, Halbhuber K-J, von Banchet GS. The proportion of
599 TRPV1 protein-positive lumbar DRG neurones does not increase in the course of acute
600 and chronic antigen-induced arthritis in the knee joint of the rat. Neuroscience Letters
601 2004;361:172–175.

602 [5] Behrendt H-J, Germann T, Gillen C, Hatt H, Jostock R. Characterization of the mouse
603 cold-menthol receptor TRPM8 and vanilloid receptor type-1 VR1 using a fluorometric
604 imaging plate reader (FLIPR) assay. British Journal of Pharmacology 2004;141:737–745.

605 [6] Bonet IJM, Fischer L, Parada CA, Tambeli CH. The role of transient receptor potential A
606 1 (TRPA1) in the development and maintenance of carrageenan-induced hyperalgesia.
607 Neuropharmacology 2013;65:206–212.

608 [7] Brandt MR, Beyer CE, Stahl SM. TRPV1 Antagonists and Chronic Pain: Beyond Thermal
609 Perception. Pharmaceuticals 2012;5:114–132.

610 [8] Caceres AI, Liu B, Jabba SV, Achanta S, Morris JB, Jordt S. Transient Receptor Potential
611 Cation Channel Subfamily M Member 8 channels mediate the anti-inflammatory effects of
612 eucalyptol. British Journal of Pharmacology 2017;174:867–879.

613 [9] Cervero F, Laird JMA, García-Nicas E. Secondary hyperalgesia and presynaptic
614 inhibition: an update. European Journal of Pain 2003;7:345–351.

615 [10] Chebib M, Johnston GAR. The “ABC” of GABA receptors: a brief overview. Clinical and
616 Experimental Pharmacology and Physiology 2001;26:937–940.

617 [11] Chen W, Walwyn W, Ennes HS, Kim H, McRoberts JA, Marvizón JCG. BDNF released
618 during neuropathic pain potentiates NMDA receptors in primary afferent terminals. The
619 European journal of neuroscience 2014;39:1439–1454.

620 [12] Chen Y, Willcockson HH, Valtschanoff JG. Vanilloid receptor TRPV1-mediated
621 phosphorylation of ERK in murine adjuvant arthritis. Osteoarthritis and Cartilage
622 2009;17:244–251.

[13] Cho WG, Valtschanoff JG. Vanilloid receptor TRPV1-positive sensory afferents in the mouse ankle and knee joints. Brain Research 2008;1219:59–65.

[14] Davis JB, Gray J, Gunthorpe MJ, Hatcher JP, Davey PT, Overend P, Harries MH, Latcham J, Clapham C, Atkinson K, Hughes SA, Rance K, Grau E, Harper AJ, Pugh PL, Rogers DC, Bingham S, Randall A, Sheardown SA. Vanilloid receptor-1 is essential for inflammatory thermal hyperalgesia. Nature 2000;405:183.

[15] Deacon RMJ. Digging and marble burying in mice: simple methods for in vivo identification of biological impacts. Nature Protocols 2006;1:122.

[16] Djouhri L, Bleazard L, Lawson SN. Association of somatic action potential shape with sensory receptive properties in guinea-pig dorsal root ganglion neurones. The Journal of Physiology 1998;513:857–872.

[17] Djouhri L, Lawson SN. Changes in somatic action potential shape in guinea-pig nociceptive primary afferent neurones during inflammation in vivo. The Journal of Physiology 1999;520:565–576.

[18] Farr M, Garvey K, Bold AM, Kendall MJ, Bacon PA. Significance of the hydrogen ion concentration in synovial fluid in rheumatoid arthritis. Clin Exp Rheumatol 1985;3:99–104.

[19] Fernandes ES, Russell FA, Alawi KM, Sand C, Liang L, Salamon R, Bodkin JV, Aubdool AA, Arno M, Gentry C, Smillie S-J, Bevan S, Keeble JE, Malcangio M, Brain SD. Environmental cold exposure increases blood flow and affects pain sensitivity in the knee joints of CFA-induced arthritic mice in a TRPA1-dependent manner. Arthritis Research & Therapy 2016;18:7.

[20] Fernandes ES, Russell FA, Spina D, McDougall JJ, Graepel R, Gentry C, Staniland AA, Mountford DM, Keeble JE, Malcangio M, Bevan S, Brain SD. A Distinct Role for Transient Receptor Potential Ankyrin 1, in Addition to Transient Receptor Potential Vanilloid 1, in Tumor Necrosis Factor alpha-Induced Inflammatory Hyperalgesia and Freund's Complete Adjuvant-Induced Monarthritis. Arthritis and Rheumatism 2011;63:819–829.

[21] Fernandes ES, S A, R K, Brain S. TRP Receptors in Arthritis, Gaining Knowledge for Translation from Experimental Models. 2013 p.

[22] Flake NM, Gold MS. Inflammation alters sodium currents and excitability of temporomandibular joint afferents. Neuroscience Letters 2005;384:294–299.

[23] Fujii W, Kawahito Y, Nagahara H, Kukida Y, Seno T, Yamamoto A, Kohno M, Oda R, Taniguchi D, Fujiwara H, Ejima A, Kishida T, Mazda O, Ashihara E. Monocarboxylate Transporter 4, Associated With the Acidification of Synovial Fluid, Is a Novel Therapeutic Target for Inflammatory Arthritis. Arthritis & Rheumatology 2015;67:2888–2896.

660 [24] Gareth J. Treharne, George D. Kitas, Antonia C. Lyons, David A. Booth. Well-being in
661 Rheumatoid Arthritis: The Effects of Disease Duration and Psychosocial
662 Factors. J Health Psychol 2005;10:457–474.

663 [25] Garrison SR, Stucky CL. Contribution of Transient Receptor Potential Ankyrin 1 to
664 Chronic Pain in Aged Mice With Complete Freund's Adjuvant–Induced Arthritis.
665 Arthritis & Rheumatology 2014;66:2380–2390.

666 [26] Gauldie SD, McQueen DS, Clarke CJ, Chessell IP. A robust model of adjuvant-induced
667 chronic unilateral arthritis in two mouse strains. J Neurosci Methods 2004;139:281–291.

668 [27] Grubb BD, Birrell GJ, McQueen DS, Iggo A. The role of PGE2 in the sensitization of
669 mechanoreceptors in normal and inflamed ankle joints of the rat. Experimental Brain
670 Research 1991;84:383–392.

671 [28] Hannan MT. Epidemiologic perspectives on women and arthritis: An overview. Arthritis
672 & Rheumatism 1996;9:424–434.

673 [29] Hawker GA, Stewart L, French MR, Cibere J, Jordan JM, March L, Suarez-Almazor M,
674 Gooberman-Hill R. Understanding the pain experience in hip and knee osteoarthritis – an
675 OARSI/OMERACT initiative. Osteoarthritis and Cartilage n.d.;16:415–422.

676 [30] Haywood AR, Hathway GJ, Chapman V. Differential contributions of peripheral and
677 central mechanisms to pain in a rodent model of osteoarthritis. Scientific Reports
678 2018;8:7122.

679 [31] Hillery CA, Kerstein PC, Vilceanu D, Barabas ME, Retherford D, Brandow AM,
680 Wandersee NJ, Stucky CL. Transient receptor potential vanilloid 1 mediates pain in mice
681 with severe sickle cell disease. Blood 2011;118:3376–3383.

682 [32] Hockley JRF, Taylor TS, Callejo G, Wilbrey AL, Gutteridge A, Bach K, Winchester WJ,
683 Bulmer DC, McMurray G, Smith ESJ. Single-cell RNAseq reveals seven classes of
684 colonic sensory neuron. Gut 2018. doi:10.1136/gutjnl-2017-315631.

685 [33] Holzer P. Acid-sensitive ion channels and receptors. Handbook of experimental
686 pharmacology 2009:283–332.

687 [34] Honore P, Wismer CT, Mikusa J, Zhu CZ, Zhong C, Gauvin DM, Gomtsyan A, El
688 Kouhen R, Lee C-H, Marsh K, Sullivan JP, Faltynek CR, Jarvis MF. A-425619 [1-
689 Isoquinolin-5-yl-3-(4-trifluoromethyl-benzyl)-urea], a Novel Transient Receptor Potential
690 Type V1 Receptor Antagonist, Relieves Pathophysiological Pain Associated with
691 Inflammation and Tissue Injury in Rats. J Pharmacol Exp Ther 2005;314:410.

692 [35] Hsieh W-S, Kung C-C, Huang S-L, Lin S-C, Sun W-H. TDAG8, TRPV1, and ASIC3
693 involved in establishing hyperalgesic priming in experimental rheumatoid arthritis.
694 Scientific Reports 2017;7:8870.

695 [36] Ikeuchi M, Kolker SJ, Sluka KA. Acid-sensing ion channel 3 expression in mouse knee
696 joint afferents and effects of carrageenan-induced arthritis. J Pain 2009;10.
697 doi:10.1016/j.jpain.2008.10.010.

698 [37] Ji R-R, Samad TA, Jin S-X, Schmoll R, Woolf CJ. p38 MAPK Activation by NGF in
699 Primary Sensory Neurons after Inflammation Increases TRPV1 Levels and Maintains Heat
700 Hyperalgesia. Neuron 2002;36:57–68.

701 [38] Jirkof P. Burrowing and nest building behavior as indicators of well-being in mice.
702 Journal of Neuroscience Methods 2014;234:139–146.

703 [39] Keeble J, Russell F, Curtis B, Starr A, Pinter E, Brain SD. Involvement of transient
704 receptor potential vanilloid 1 in the vascular and hyperalgesic components of joint
705 inflammation. Arthritis and Rheumatism 2005;52:3248–3256.

706 [40] Lawson SN, McCarthy PW, Prabhakar E. Electrophysiological properties of neurones
707 with CGRP-like immunoreactivity in rat dorsal root ganglia. Journal of Comparative
708 Neurology 1996;365:355–366.

709 [41] Lee KY, Charbonnet M, Gold MS. Upregulation of high affinity GABA(A) receptors in
710 cultured rat dorsal root ganglion neurons. Neuroscience 2012;208C:133–142.

711 [42] Lewis T. Study of Somatic Pain. British Medical Journal 1938;1:321–325.

712 [43] Li C-L, Li K-C, Wu D, Chen Y, Luo H, Zhao J-R, Wang S-S, Sun M-M, Lu Y-J, Zhong
713 Y-Q, Hu X-Y, Hou R, Zhou B-B, Bao L, Xiao H-S, Zhang X. Somatosensory neuron
714 types identified by high-coverage single-cell RNA-sequencing and functional
715 heterogeneity. Cell Research 2015;26:83.

716 [44] Moilanen LJ, Laavola M, Kukkonen M, Korhonen R, Leppänen T, Högestätt ED,
717 Zygmunt PM, Nieminen RM, Moilanen E. TRPA1 Contributes to the Acute Inflammatory
718 Response and Mediates Carrageenan-Induced Paw Edema in the Mouse. Scientific
719 Reports 2012;2:380.

720 [45] Moore C, Gupta R, Jordt S-E, Chen Y, Liedtke WB. Regulation of Pain and Itch by TRP
721 Channels. Neuroscience Bulletin 2018;34:120–142.

722 [46] Petrus M, Peier AM, Bandell M, Hwang SW, Huynh T, Olney N, Jegla T, Patapoutian A.
723 A role of TRPA1 in mechanical hyperalgesia is revealed by pharmacological inhibition.
724 Molecular Pain 2007;3:40–40.

725 [47] Price MP, McIlwrath SL, Xie J, Cheng C, Qiao J, Tarr DE, Sluka KA, Brennan TJ, Lewin
726 GR, Welsh MJ. The DRASIC Cation Channel contributes to the detection of cutaneous
727 touch and acid stimuli in mice. Neuron 2001;32. doi:10.1016/S0896-6273(01)00547-5.

728 [48] Rice ASC, Cimino-Brown D, Eisenach JC, Kontinen VK, Lacroix-Fralish ML, Machin I,
729 Mogil JS, Stöhr T. Animal models and the prediction of efficacy in clinical trials of

730 analgesic drugs: A critical appraisal and call for uniform reporting standards. PAIN
731 2008;139:243–247.

732 [49] Rigaud M, Gemes G, Barabas M-E, Chernoff DI, Abram SE, Stucky CL, Hogan QH.
733 Species and strain differences in rodent sciatic nerve anatomy: Implications for studies of
734 neuropathic pain. Pain 2008;136:188–201.

735 [50] Rutten K, Robens A, Read SJ, Christoph T. Pharmacological validation of a refined
736 burrowing paradigm for prediction of analgesic efficacy in a rat model of sub-chronic
737 knee joint inflammation. European Journal of Pain 2014;18:213–222.

738 [51] Samer R Eid, Eric D Crown, Eric L Moore, Hongyu A Liang, Kar-Chan Choong, Shelley
739 Dima, Darrell A Henze, Stefanie A Kane, Mark O Urban. HC-030031, a TRPA1 Selective
740 Antagonist, Attenuates Inflammatory- and Neuropathy-Induced Mechanical
741 Hypersensitivity. Mol Pain 2008;4:1744-8069-4–48.

742 [52] Sara Nencini, Mitchell Ringuet, Dong-Hyun Kim, Yu-Jen Chen, Claire Greenhill, Jason J
743 Ivanusic. Mechanisms of nerve growth factor signaling in bone nociceptors and in an
744 animal model of inflammatory bone pain. Mol Pain 2017;13:1744806917697011.

745 [53] Schaible H-G, Ebersberger A, von Banchet GS. Mechanisms of Pain in Arthritis. Annals
746 of the New York Academy of Sciences 2002;966:343–354.

747 [54] Scott BS, Edwards BA. Electric membrane properties of adult mouse DRG neurons and
748 the effect of culture duration. J Neurobiol 1980;11:291–301.

749 [55] Seidel MF, Wise BL, Lane NE. Nerve growth factor: an update on the science and
750 therapy. Osteoarthritis and Cartilage 2013;21:1223–1228.

751 [56] da Silva Serra I, Husson Z, Bartlett JD, Smith ES. Characterization of cutaneous and
752 articular sensory neurons. LID - 10.1177/1744806916636387 [doi] LID -
753 1744806916636387 [pii]. 2016.

754 [57] Sluka KA, Price MP, Breese NM, Stucky CL, Wemmie JA, Welsh MJ. Chronic
755 hyperalgesia induced by repeated acid injections in muscle is abolished by the loss of
756 ASIC3, but not ASIC1. Pain 2003;106. doi:10.1016/S0304-3959(03)00269-0.

757 [58] Smith ESJ, Omerbašić D, Lechner SG, Anirudhan G, Lapatsina L, Lewin GR. The
758 Molecular Basis of Acid Insensitivity in the African Naked Mole-Rat. Science
759 2011;334:1557.

760 [59] St. John Smith E. Advances in understanding nociception and neuropathic pain. Journal of
761 Neurology 2018;265:231–238.

762 [60] Staniland AA, McMahon SB. Mice lacking acid-sensing ion channels (ASIC) 1 or 2, but
763 not ASIC3, show increased pain behaviour in the formalin test. European Journal of Pain
764 2009;13:554–563.

765 [61] Story GM, Peier AM, Reeve AJ, Eid SR, Mosbacher J, Hricik TR, Earley TJ, Hergarden
766 AC, Andersson DA, Hwang SW, McIntyre P, Jegla T, Bevan S, Patapoutian A.
767 ANKTM1, a TRP-like Channel Expressed in Nociceptive Neurons, Is Activated by Cold
768 Temperatures. Cell 2003;112:819–829.

769 [62] Sung K-W, Kirby M, McDonald MP, Lovinger DM, Delpire E. Abnormal $GABA_A$
770 Receptor-Mediated Currents in Dorsal Root Ganglion Neurons Isolated from Na–K–2Cl
771 Cotransporter Null Mice. J. Neurosci. 2000;20:7531.

772 [63] Sutherland FI, Bannatyne BA, Kerr R, Riddell JS, Maxwell DJ. Inhibitory amino acid
773 transmitters associated with axons in presynaptic apposition to cutaneous primary afferent
774 axons in the cat spinal cord. J Comp Neurol 2002;452:154–162.

775 [64] Usoskin D, Furlan A, Islam S, Abdo H, Lonnerberg P, Lou D, Hjerling-Leffler J,
776 Haeggstrom J, Kharchenko O, Kharchenko PV, Linnarsson S, Ernfors P. Unbiased
777 classification of sensory neuron types by large-scale single-cell RNA sequencing. Nat
778 Neurosci 2015;18:145–153.

779 [65] Vilen L, Baldassari AR, Callahan LF. Socioeconomic burden of pain in rheumatic disease.
780 Clin Exp Rheumatol 2017;35 Suppl 107:26–31.

781 [66] Weng X, Smith T, Sathish J, Djouhri L. Chronic inflammatory pain is associated with
782 increased excitability and hyperpolarization-activated current (Ih) in C- but not Aδ-
783 nociceptors. PAIN® 2012;153:900–914.

784 [67] Willis WDJ. Dorsal root potentials and dorsal root reflexes: a double-edged sword. Exp
785 Brain Res 1999;124:395–421.

786 [68] Winter J, Alistair Forbes C, Sternberg J, Lindsay RM. Nerve growth factor (NGF)
787 regulates adult rat cultured dorsal root ganglion neuron responses to the excitotoxin
788 capsaicin. Neuron 1988;1:973–981.

789 [69] Wright AJ, Husson ZMA, Hu D-E, Callejo G, Brindle KM, Smith ESJ. Increased
790 hyperpolarized [1-13C] lactate production in a model of joint inflammation is not
791 accompanied by tissue acidosis as assessed using hyperpolarized 13C-labelled
792 bicarbonate. NMR in Biomedicine n.d.:e3892–n/a.

793 [70] Yu L, Yang F, Luo H, Liu FY, Han JS, Xing GG, Wan Y. The role of TRPV1 in different
794 subtypes of dorsal root ganglion neurons in rat chronic inflammatory nociception induced
795 by complete Freund's adjuvant. Mol Pain 2008;4. doi:10.1186/1744-8069-4-61.

796 [71] Zhang R-X, Ren K, Dubner R. Osteoarthritis pain mechanisms: Basic studies in animal
797 models. Osteoarthritis and cartilage / OARS, Osteoarthritis Research Society
798 2013;21:1308–1315.

799 [72] Zhang X, Huang J, McNaughton PA. NGF rapidly increases membrane expression of
800 TRPV1 heat-gated ion channels. EMBO J 2005;24:4211.

[73] Zhang X, Lee K-Y, Priest BT, Belfer I, Gold MS. Inflammatory mediator-induced modulation of GABA(A) currents in human sensory neurons. Neuroscience 2015;310:401–409.

[74] Zhou Y, Li G-D, Zhao Z-Q. State-dependent phosphorylation of ε-isozyme of protein kinase C in adult rat dorsal root ganglia after inflammation and nerve injury. Journal of Neurochemistry 2003;85:571–580.

[75] Zhu Y, Lu S, Gold MS. Persistent inflammation increases GABA-induced depolarization of rat cutaneous dorsal root ganglion neurons in vitro. Neuroscience 2012;220:330–340.

Figure Legends:

Figure 1: CFA model of acute knee inflammation in mice. A) Experimental timeline indicating when intra-articular injections, behavioral training and measurements were conducted. B) Representative picture of CFA injected (ipsilateral) and non-injected (contralateral) knee (shaved before injections). Arrows indicate where knee width was measured. C) Knee width on the day of CFA injection (pre) and 24-hours after CFA injection (post) in the ipsilateral (red dots) and contralateral (black dots) knee (n =17). **** indicates $p < 0.0001$, paired t-test. Plots of (D) time spent digging and (E) the number of visible burrows after a 3-minute digging test (n = 7). * indicates $p < 0.05$, ** indicates $p < 0.01$, repeated measures ANOVA, Holm-Sidak multiple comparison test. Error bars indicate S.D.

825

826 Figure 2: Action potential properties of knee neurons following acute knee inflammation. A)
827 Evoked action potential from a knee neuron in response to a 700 pA current injection for 80 ms.
828 Example of a labeled knee neuron (blue arrow) and an unlabeled neuron (white arrow) shown in
829 inset. B) Frequency distribution of neuronal diameter in μm of CFA (red, n = 25) and Cntrl (black,
830 n = 27) neurons. C-E) Distribution of threshold (C), half peak duration (HPD) (D) and
831 afterhyperpolarization (AHP) (E) after 4-hours in culture. Error bars indicate S.D, * indicates $p <$
832 0.05, ** indicates $p < 0.01$, unpaired t-test.

833

834 Figure 3: Acid sensitivity of knee neurons after acute inflammation. A) Percentage frequency of
835 transient + sustained vs. sustained only response to pH 6 (transient + sustained, light yellow;
836 sustained, dark yellow) and pH 5 (transient + sustained, light orange; sustained, orange) B)
837 Example traces of transient + sustained acid currents in response to pH 6 (light yellow) and pH 5
838 (light orange). C) Example traces of sustained response to pH 7 (purple), pH 6 (dark yellow) and
839 pH 5 (orange). D-F) Peak current density of sustained pH 7 (n = 19, 23), pH 6 (n = 23, 25) and
840 pH 5 (n = 20, 23) responses (CFA: red dots, Cntrl: black dots).

841

842 Figure 4: TRP agonist response profile of knee neurons following acute knee inflammation.
843 Representative traces of 10 μM capsaicin (pink, Ai), 100 μM cinnamaldehyde (brown, Bi) and
844 100 μM menthol (green, Ci) response from a CFA neuron and their respective percentage
845 frequency (Aii, Bii, Cii). The numbers above the bars indicate the number of responsive neurons.
846 D) Heat map of Cntrl (i, n = 27) and CFA (ii, n = 25) neurons responding to capsaicin,

847 cinnamaldehyde and menthol. E (i) Representative images of a whole DRG section from L4
848 showing fast blue (FB) labeling from the knee (blue), TRPV1 expression (magenta), TrkA
849 expression (green) and a merged image. White arrowhead shows a knee neuron that only expresses
850 TrkA, white arrowhead with asterisk shows a knee neuron that expresses only TRPV1 and white
851 arrow shows a knee neuron that co-expresses TRPV1 and TrkA. (ii) Proportion of knee neurons
852 (L2-L5) that express TRPV1 (magenta), TrkA (green) and both TRPV1 and TrkA (green and
853 magenta stripes) from Cntrl (n = 1334) and CFA (n = 1089) injected side. Numbers above the bars
854 represent neurons stained positive with respective antibodies. * indicates $p < 0.05$, **** indicates
855 $p < 0.0001$, chi-sq test.

856

857 Figure 5: GABA-evoked currents from knee neurons after acute inflammation. A) Representative
858 traces of 100 μM GABA-evoked currents showing both transient and sustained phases (i, ii) and
859 currents with only a sustained phase (iii). B (i) Percentage frequency of GABA-evoked transient
860 + sustained currents (black bars), sustained currents (striped bars) and non-responders (grey bars)
861 in Cntrl and CFA neurons. (ii) Peak current density of all GABA-evoked currents (Cntrl: n = 26,
862 CFA: 19) and (iii) GABA-evoked currents split into TS and S type (Cntrl: n = 12, 14, black dots;
863 CFA: n = 12, 7, red dots). TS = transient + sustained currents, S = sustained only currents, error
864 bars indicate S.D, * indicates $p < 0.05$, unpaired t-test. C) i - Example trace of bicuculline block
865 (blue) of GABA-evoked currents and THIP-evoked current (green) in a single neuron. ii –
866 percentage frequency of Cntrl (n = 11) and CFA (n = 8) neurons with a GABA response that also
867 responded to THIP. The numbers above the bars indicate the number of responsive neurons.

868

869 Figure 6: Digging behavior after injection of the TRPV1 antagonist A-425619. A) Experimental
870 timeline highlighting the days where behavioral testing and injection was performed. Distribution
871 of time spent digging and the number of burrows in the CFA (B, C, n = 10) and saline group (D,
872 E, n = 7). * indicates $p < 0.05$, ** indicates $p < 0.01$, *** indicates $p < 0.0001$. rmANOVA, Holm-
873 Sidak multiple comparison test. Error bars indicate S.D.

874

875 Supplementary Digital Content 1: Video that shows a mouse digging after FB injection in the knee
876 (left) and after CFA injection in the knee (right).mp4

877

878 Supplementary Digital Content 2: Figure showing time-in-culture effects on acid, TRP agonist and
879 GABA sensitivity of knee neurons after inflammation.pdf

880 A) Proportion of Cntrl (left) and CFA (right) neurons responding to pH 6 (yellow) and pH 5
881 (orange) with a transient + sustained type current (light shade) and sustained only type current
882 (dark shade) across 4, 24 and 48-hours. B) Percentage frequency of Cntrl (left) and CFA (right)
883 neurons sensitive to capsaicin (pink), cinnamaldehyde (brown) and menthol (green) across 4, 24
884 and 48-hours in culture. C) Percentage of Cntrl (left) and CFA (right) neurons that had a sustained
885 GABA-evoked current across 4, 24 and 48-hours in culture. * indicates $p < 0.05$, chi-sq test. The
886 numbers above the bars indicate number of responsive neurons.

Table 1: Properties of knee-innervating dorsal root ganglion neurons from the CFA injected side (CFA) and contralateral side (Cntrl) across time-in-culture. * = significance test of CFA vs Cntrl neurons in the same time group by unpaired t-test, # = significance test of CFA neurons amongst the three time points by ANOVA, ^ = significance test of Cntrl neurons amongst the three time points by ANOVA. */#/^ indicates $p < 0.05$, **/##/^^^ indicates $p < 0.01$, ***/###/^^^ indicates $p < 0.0001$.

	4-hours				24-hours				48-hours			
	CFA (n = 25)		Cntrl (n = 27)		CFA (n = 25)		Cntrl (n = 22)		CFA (n = 23)		Cntrl (n = 22)	
	Mean	S.D.	Mean	S.D.	Mean	S.D.	Mean	S.D.	Mean	S.D.	Mean	S.D.
RMP (mV)	-55.7	10.3	-58.3	8.6	-55.3	6.9	-52.5	9.0	-55.6	6.4	-54.6	8.6
Diameter (µm)	31.5	3.4	31.9	2.7	31.6	3.7	32.6	4.0	29.2	4.4	29.1	5.2
Capacitance (pF)	45.7	21.5	58.2	21.8	53.8	28.1	52.9	37.6	36.2	22.8	48.5	30.7
Threshold (pA)	384.0	221.6	550.0*	250.8	473.6	214.3	682.7**	225.5	552.2	225.5	475.5	316.5
Half peak duration (HPD, ms)	1.3	0.9	1.0	0.7	1.0	0.9	1.7	1.3	2.1##	1.9	2.6^^^	2.0
Afterhypolarization (AHP, ms)	8.6**	5.3	4.9	4.3	10.8	10.2	7.9	7.1	10.9	9.2	14.3^^^	10.2
Amplitude (mV)	88.2	24.2	86.2	23.7	79.3	25.4	68.3	30.0	82.7	22.2	83.1	26.0

Table 2: Sustained peak current densities of CFA and Cntrl DRG neurons in response to acid, TRP channel agonists (capsaisin, cinnamaldehyde and menthol) and GABA across time-in-culture. * = significance test of CFA vs. Cntrl neurons by unpaired t-test, # = significance test of CFA neurons amongst the three time points by ANOVA, ^ = significance test of Cntrl neurons amongst the three time points by ANOVA. #/^/* indicates $p < 0.05$, ##/^^^ indicates $p < 0.01$, ###/^^^ indicates $p < 0.0001$.

Treatment	4-hours						24-hours						48-hours					
	CFA (pA/pF)			Cntrl (pA/pF)			CFA (pA/pF)			Cntrl (pA/pF)			CFA (pA/pF)			Cntrl (pA/pF)		
	Mean	S.D.	n	Mean	S.D.	n	Mean	S.D.	n	Mean	S.D.	n	Mean	S.D.	n	Mean	S.D.	n
pH 7	1.0	1.0	19	0.6	0.3	23	4.0##	4.6	19	5.7^^^	6.4	17	1.5	1.7	15	1.5	2.7	15
pH 6	2.6	4.2	21	1.5	1.5	25	4.9	5.4	21	5.3	7.2	20	8.6	6.4	22	4.9	8.5	19
pH 5	5.3	10.4	20	2.3	1.5	23	15.5	20.2	20	14.5^^	18.4	19	7.4	6.2	19	7.9	11.6	15
Capsaicin	4.4	11.8	18	0.8	0.4	12	1.8	2.1	22	4.6	6.9	11	10.3	18.4	13	6.4	12.1	10
Cinnamaldehyde	1.1	0.8	12	0.7	0.4	18	2.2	1.9	19	2.3	2.5	14	0.9	0.8	8	2.5	4.6	5
Menthol	0.9	0.6	11	0.9	0.7	14	1.0	0.6	12	1.6	1.2	9	1.2	2.0	8	2.8	3.8	3
GABA	7.2	8.8	19	3.9	5.4	26	11.8*	12.4	22	4.3	3.9	19	8.3	11.7	18	4.3	6.7	16

Figure 1

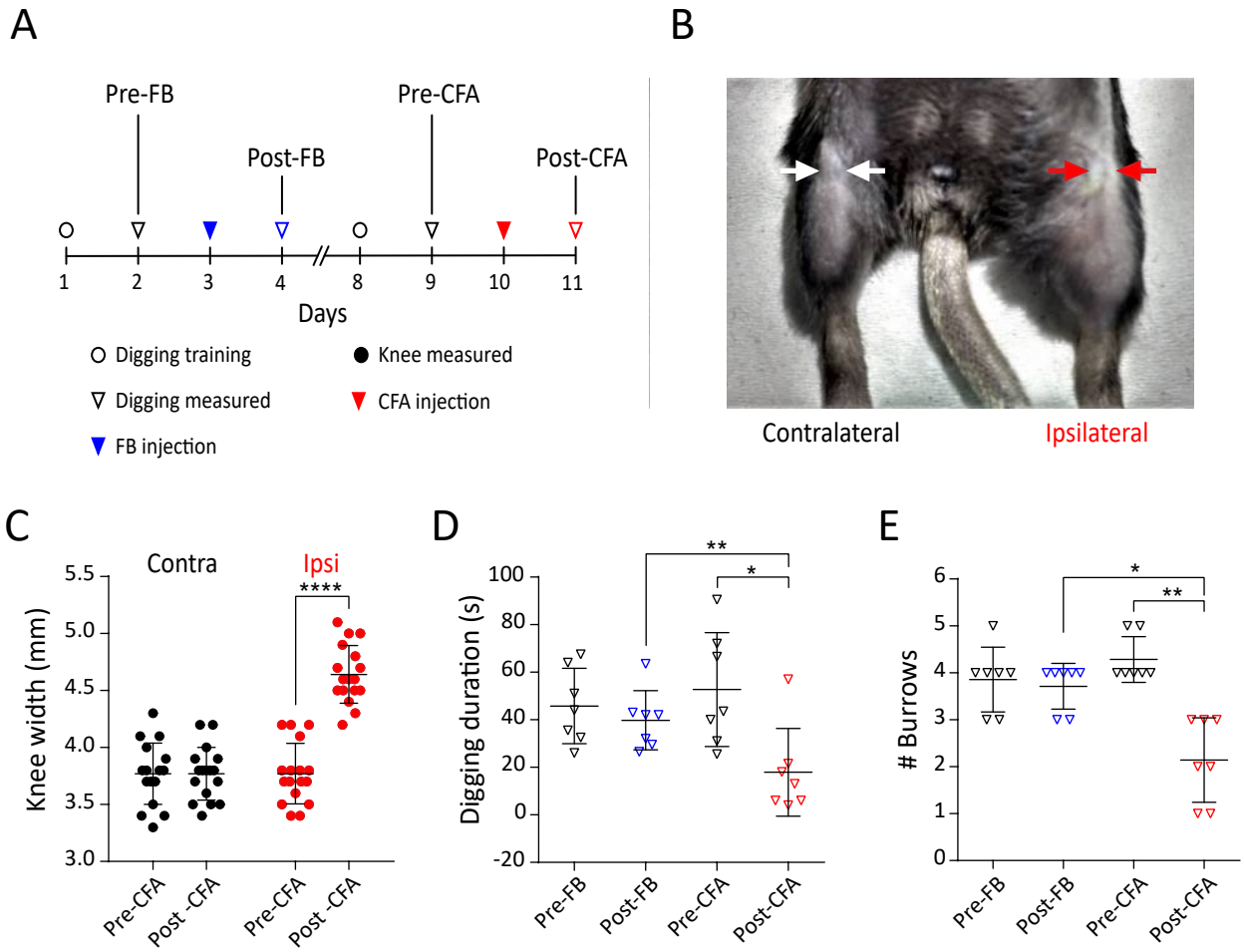
A
Pre-FB
Pre-CFA
Post-FB
Post-CFA
1
2
3
4
8
9
10
11
Days
Digging training
Knee measured
Digging measured
CFA injection
FB injection
B
Contralateral
Ipsilateral
C
Contra
Ipsi
****
Knee width (mm)
5.5
5.0
4.5
4.0
3.5
3.0
Pre-CFA
Post -CFA
Pre-CFA
Post -CFA
D
**
*
Digging duration (s)
100
80
60
40
20
0
-20
Pre-FB
Post-FB
Pre-CFA
Post-CFA
E
*
**
Burrows
6
5
4
3
2
1
0
Pre-FB
Post-FB
Pre-CFA
Post-CFA

Figure 2

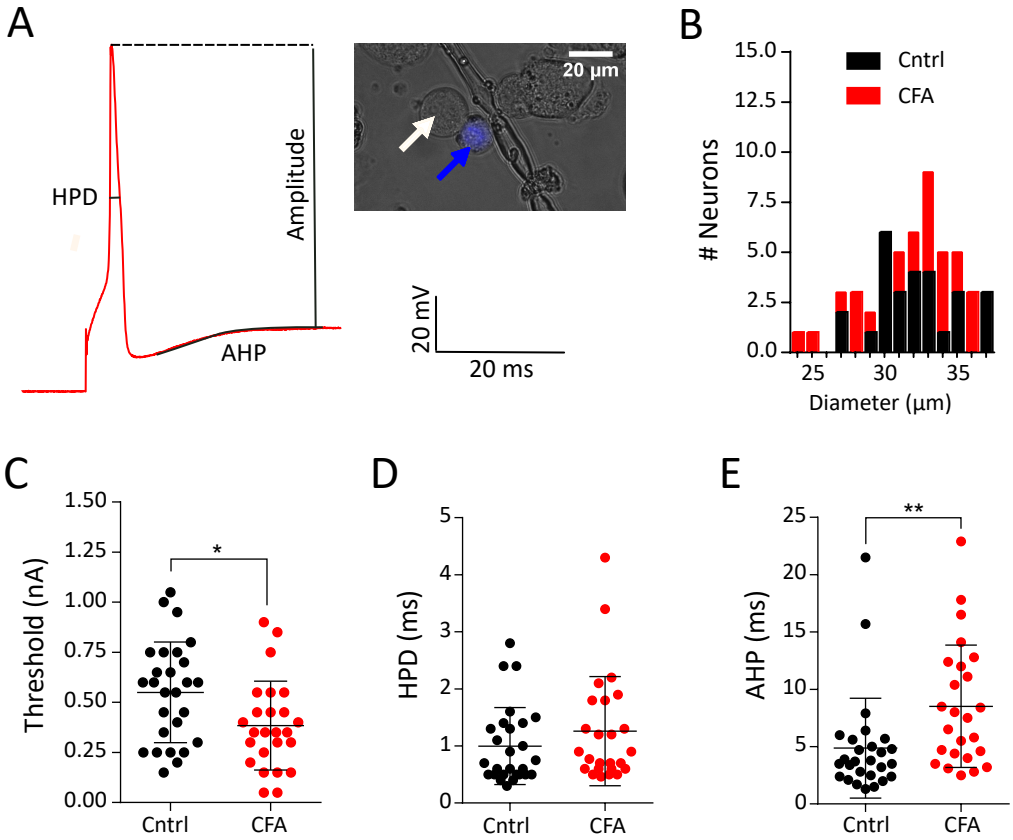
A
HPD
Amplitude
AHP
20 µm
20 mV
20 ms
B
Cntrl
CFA
Neurons
15.0
12.5
10.0
7.5
5.0
2.5
0.0
25
30
35
Diameter (µm)
C
Threshold (nA)
1.50
1.25
1.00
0.75
0.50
0.25
0.00
*
Cntrl
CFA
D
HPD (ms)
5
4
3
2
1
0
Cntrl
CFA
E
AHP (ms)
25
20
15
10
5
0
**
Cntrl
CFA

Figure 3

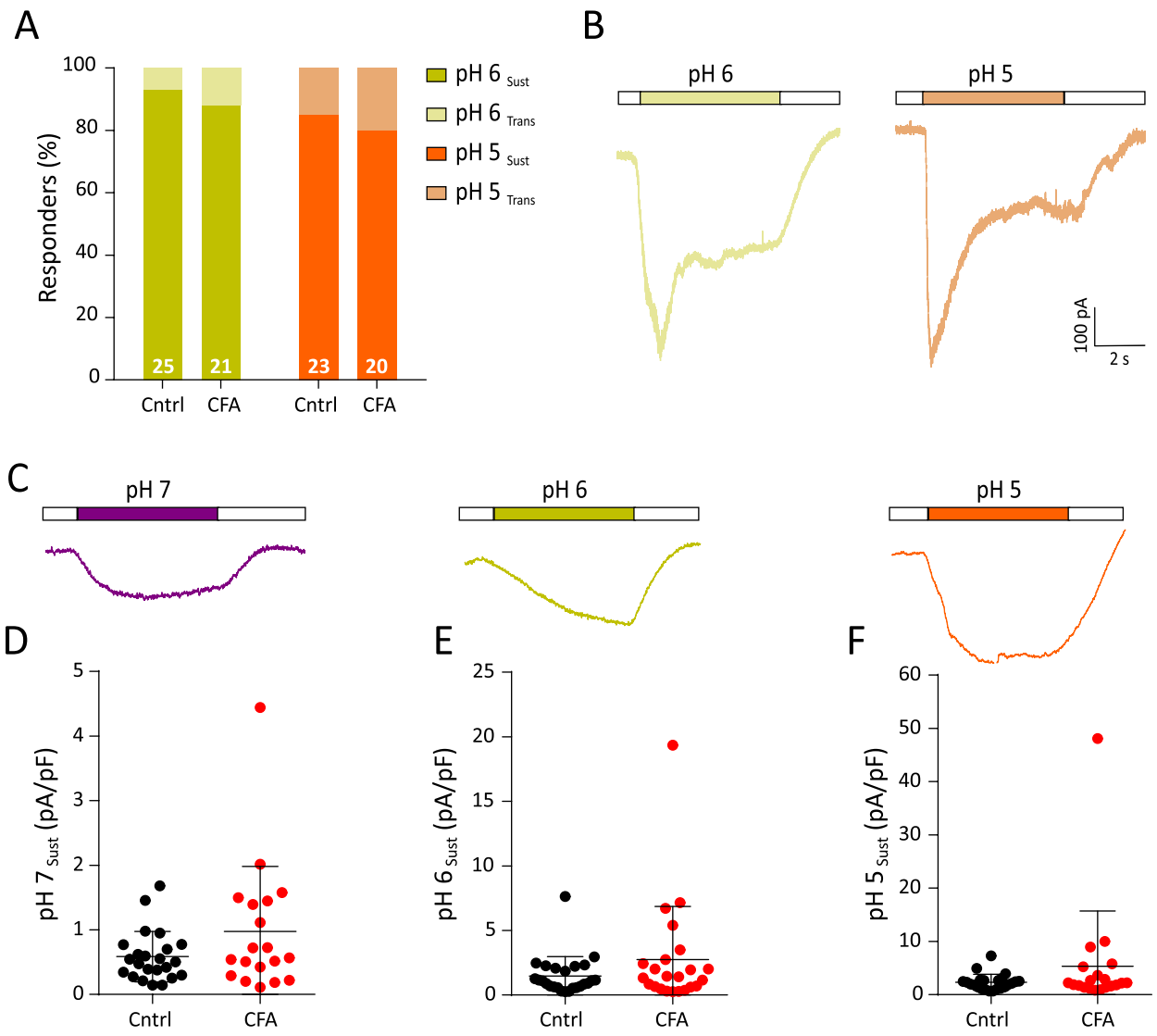
A
Responders (%)
100
80
60
40
20
0
25
21
23
20
Cntrl
CFA
Cntrl
CFA
pH 6 Sust
pH 6 Trans
pH 5 Sust
pH 5 Trans
B
pH 6
pH 5
100 pA
2 s
C
pH 7
pH 6
pH 5
D
pH 7 Sust (pA/pF)
E
pH 6 Sust (pA/pF)
F
pH 5 Sust (pA/pF)
Cntrl
CFA

Figure 4

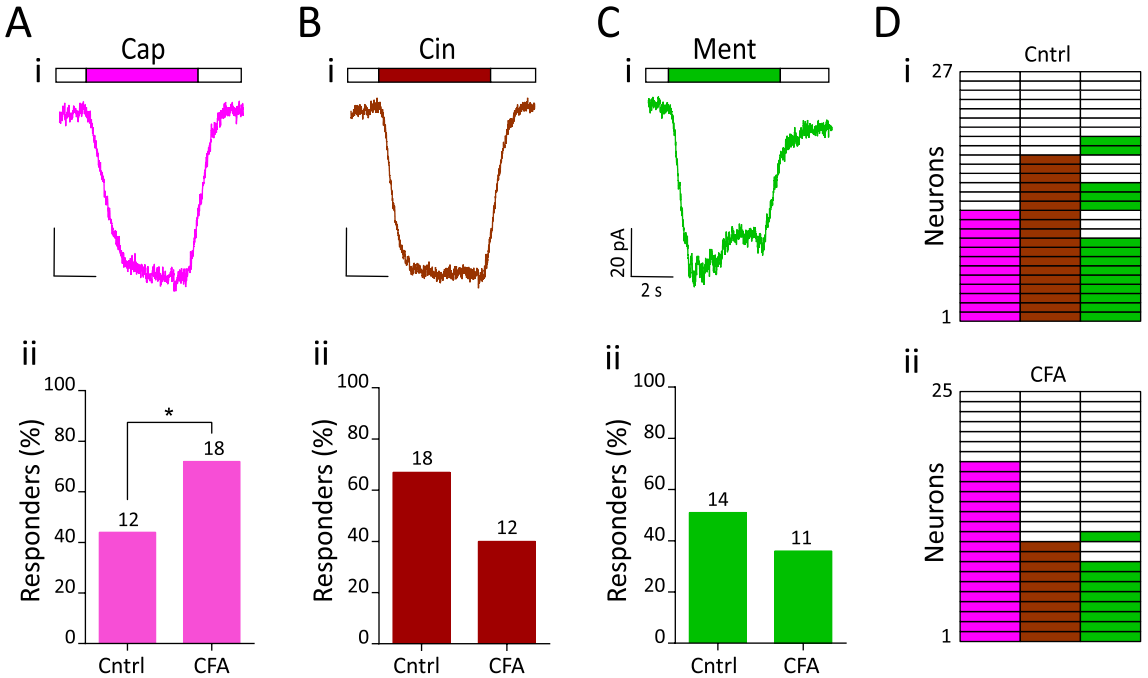
A
Cap
i
ii
Responders (%)
100
80
60
40
20
0
*
12
18
Cntrl
CFA
B
Cin
i
ii
Responders (%)
18
12
Cntrl
CFA
C
Ment
i
20 pA
2 s
ii
Responders (%)
14
11
Cntrl
CFA
D
i
Cntrl
27
Neurons
1
ii
CFA
25
Neurons
1

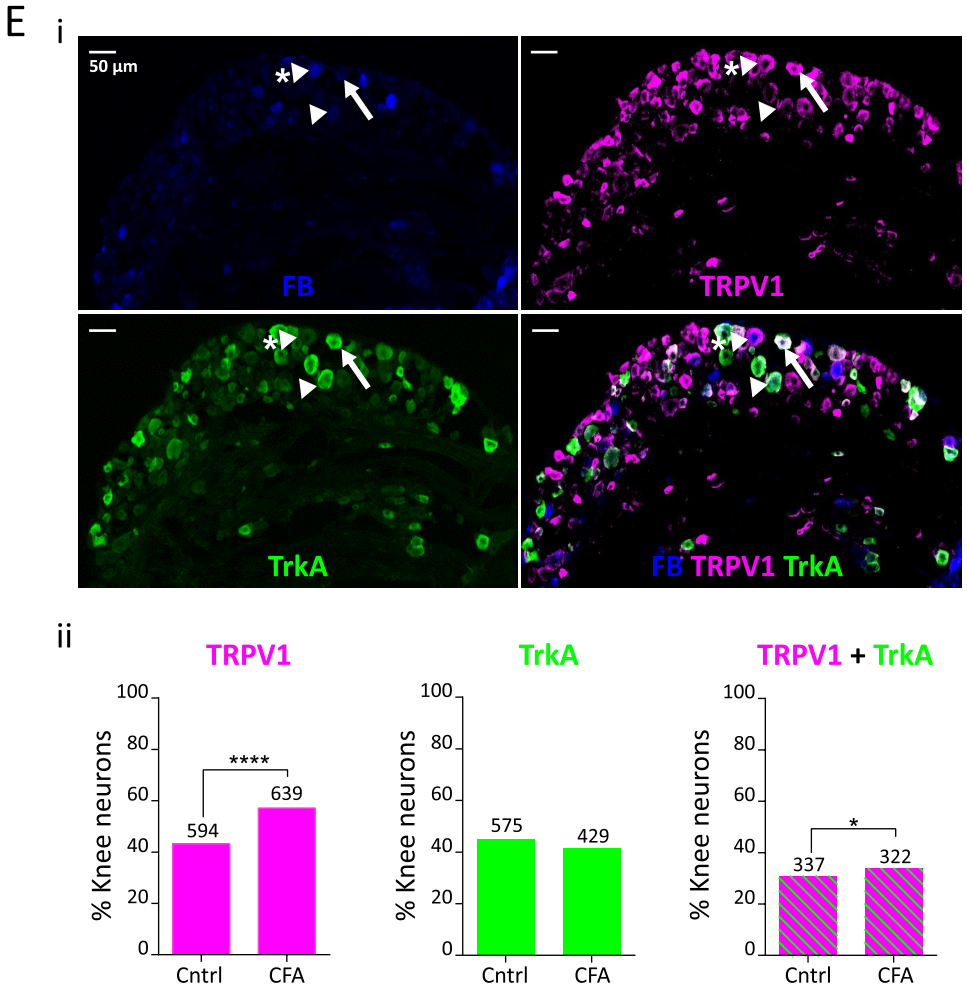
E
i
50 µm
FB
TRPV1
TrkA
FB TRPV1 TrkA
ii
TRPV1
% Knee neurons
100
80
60
40
20
0
****
594
639
Cntrl
CFA
TrkA
% Knee neurons
575
429
Cntrl
CFA
TRPV1 + TrkA
% Knee neurons
*
337
322
Cntrl
CFA

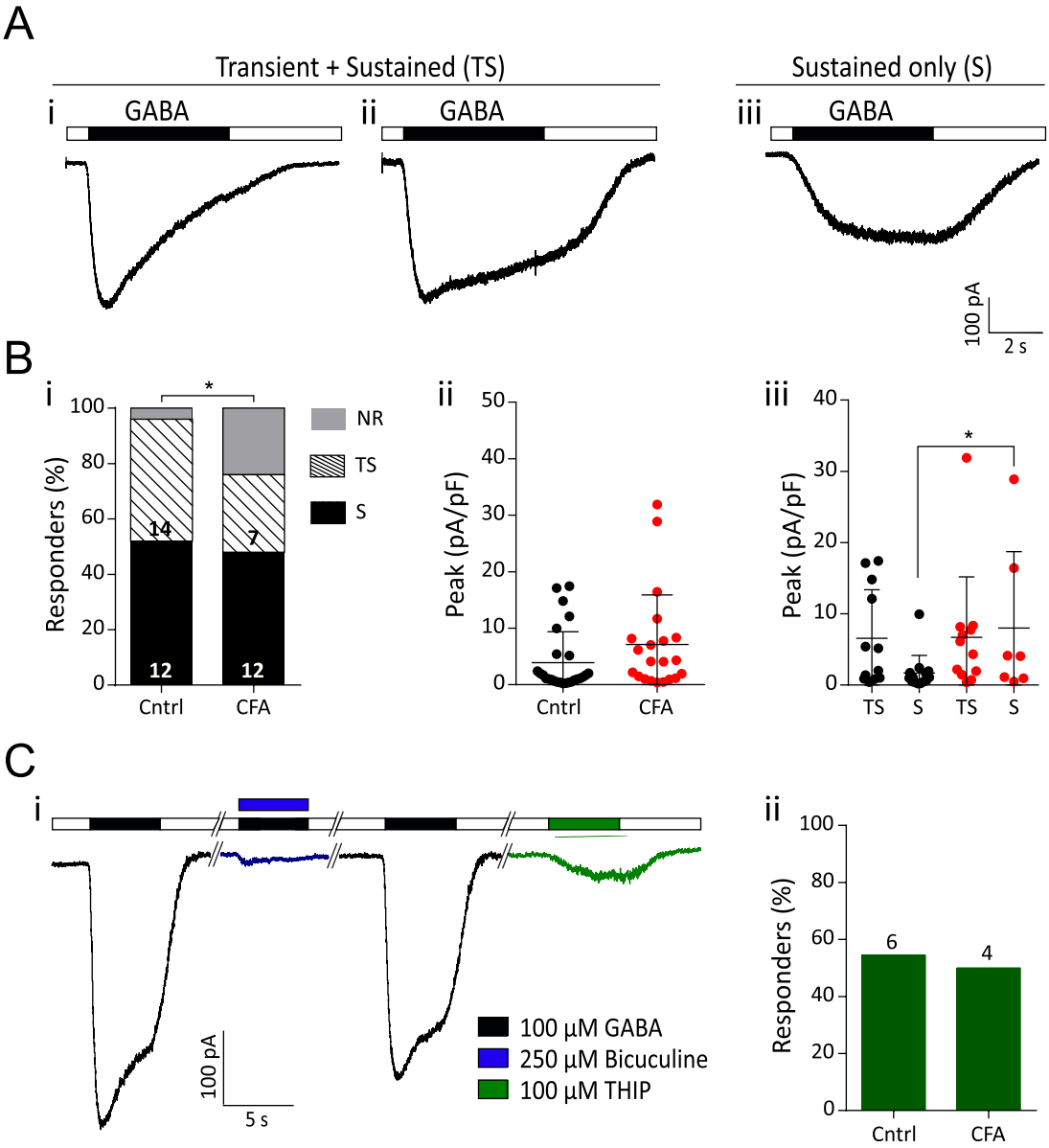
A
Transient + Sustained (TS)
Sustained only (S)
i
GABA
ii
GABA
iii
GABA
100 pA
2 s
B
i
Responders (%)
NR
TS
S
14
7
12
12
Cntrl
CFA
ii
Peak (pA/pF)
Cntrl
CFA
iii
Peak (pA/pF)
TS
S
TS
S
C
i
100 pA
5 s
100 µM GABA
250 µM Bicuculine
100 µM THIP
ii
Responders (%)
6
4
Cntrl
CFA

Figure 6

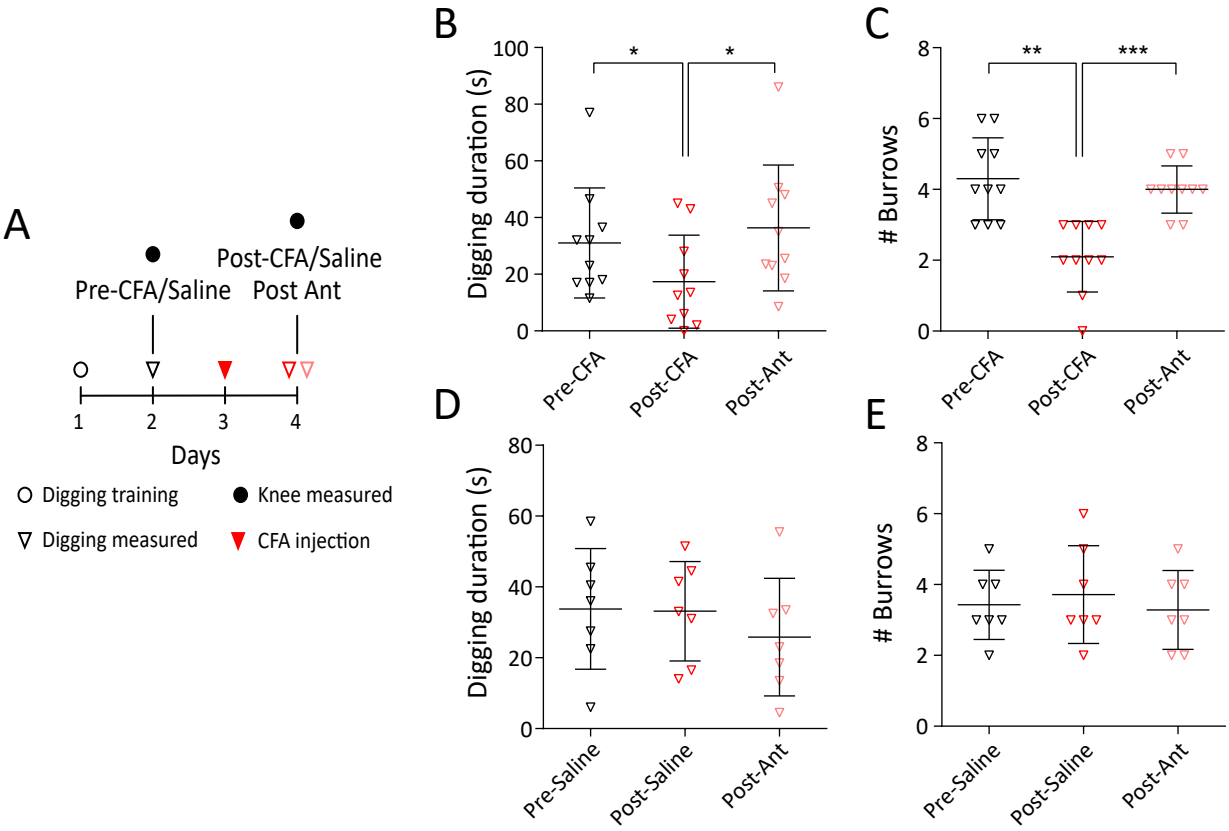
A
Pre-CFA/Saline
Post-CFA/Saline
Post Ant
1
2
3
4
Days
Digging training
Knee measured
Digging measured
CFA injection
B
Digging duration (s)
100
80
60
40
20
0
*
*
Pre-CFA
Post-CFA
Post-Ant
C
Burrows
8
6
4
2
0
**
***
Pre-CFA
Post-CFA
Post-Ant
D
Digging duration (s)
80
60
40
20
0
Pre-Saline
Post-Saline
Post-Ant
E
Burrows
8
6
4
2
0
Pre-Saline
Post-Saline
Post-Ant

Figure 6

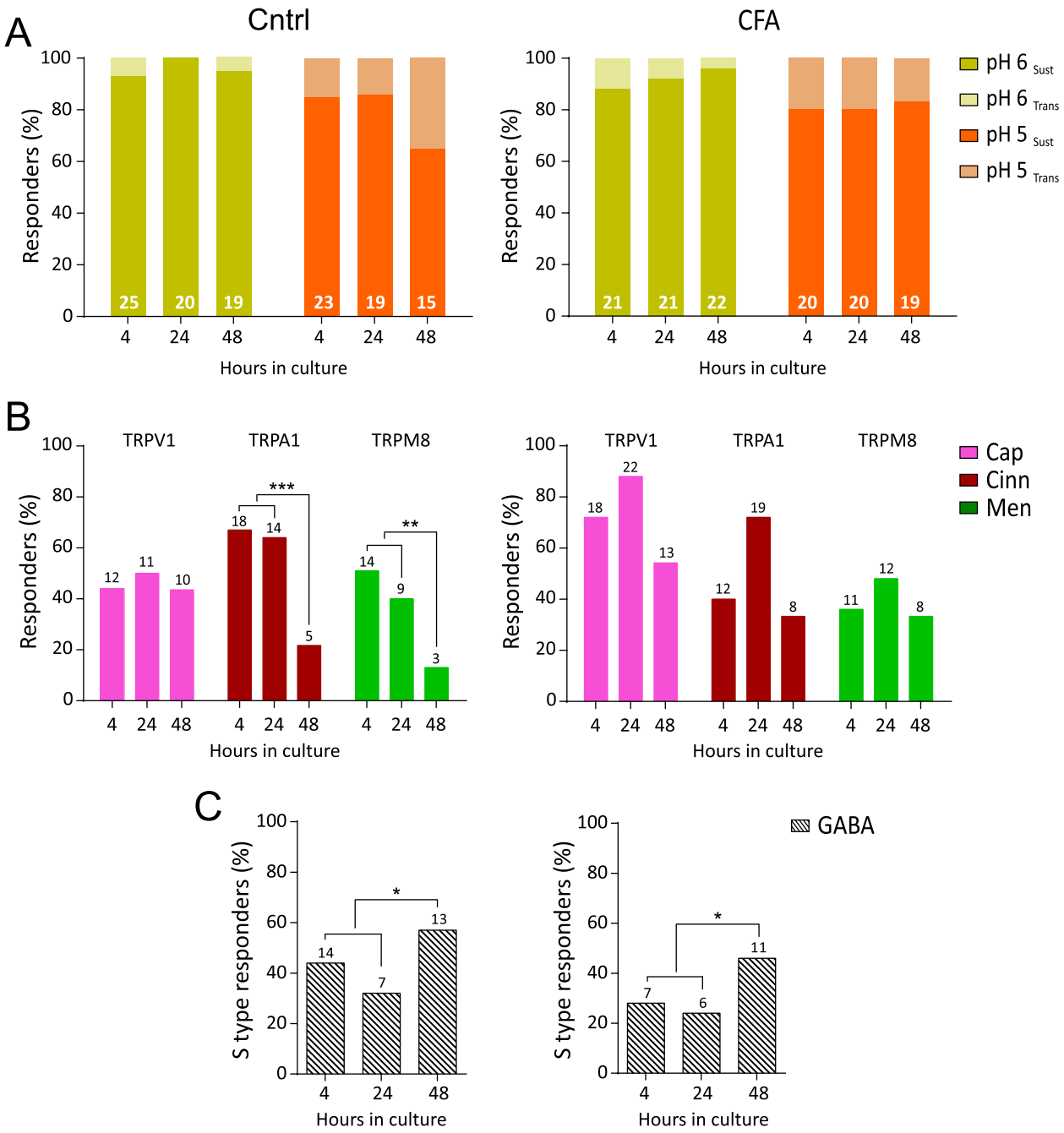
A
Cntrl
CFA
Responders (%)
Hours in culture
pH 6 Sust
pH 6 Trans
pH 5 Sust
pH 5 Trans
B
TRPV1
TRPA1
TRPM8
Cap
Cinn
Men
C
S type responders (%)
GABA